The Post-Pandemic City
Speculation Through Simulation

Michael Batty

Revised
August 8, 2021

Abstract

Although we are able to explain the way centripetal and centrifugal forces determine the form and function of historic and, to an extent, contemporary cities, our abilities to predict their futures are severely limited. The pandemic has led to changes in locational and travel behaviour as well as regulated lockdowns with respect to where people work, live and social distance from one another, and this makes it impossible to predict how we might respond to a new normal which reflects ways we are able to control and manage the pandemic. As we have little data pertaining to this future, to engage in an informed discussion, we will develop a hypothetical city which is organised according to what we know about spatial interaction, urban hierarchy, density, and heterogeneity of movement. We propose a symmetric square grid of locations, simulate the interactions using classic spatial interaction models, and then lock it down. We then release the lockdown in the transition to a new normal, assuming different parameter values controlling the effects of distance, thus illustrating how difficult it is to generate highly decentralised city forms. From this experience, we apply the model to London, again locking down the metropolis, and then exploring seven very different functional forms that provide us with a sample of different city shapes and densities. Our approach provides a framework for speculating about the future using what we call 'computable thought experiments'.

Keywords

COVID-19, spatial interaction, lockdown, working from home,
symmetry-breaking, spatial heterogeneity

Author's Note

Detailed methods and outputs used to define the hypothetical grid and London models as well as several extensive simulations of both the grid and London systems are presented in the Supplementary Information. This is referred to throughout the paper as SI.

Acknowledgements

This research is supported by The Alan Turing Institute under the QUANT2–Contract–CID–3815811, and the UK Regions Digital Research Facility (UK RDRF) EP/M023583/1.

Introduction

Cities are built up in chronological layers, regenerating from within and growing around their peripheries from without. As they grow, they generate economies of scale that increase the density of their cores (Bettencourt et al., 2007), thus accumulating key resources and services. New transportation technologies enable them to build up in heterogeneous waves around their cores as lower density suburbs. Their form and function are the result of a series of centripetal and centrifugal forces that are entangled in both simple and complex ways, where at any time the balance between locating centrally or peripherally is a precarious one (Wurster, 1963, Scott, 2019). From the first industrial revolution which began some 250 years ago, cities attracted populations from their rural hinterlands which added to their peripheral development. In the last 40 years however, there has been a slow return to the central city as the focus on automobile travel has slightly weakened and as populations have engaged in more active travel.

The pandemic has stopped all this in its tracks. Social distancing involving the 2 metre rule at the personal level has changed work, education and shopping as well as dramatically reducing mass transit, particularly rail travel. Since the pandemic began in March 2020, up to 80% of employed populations have been working from home using internet technologies (ONS, 2020), while there has been a growth in automobile travel mainly in the suburbs (Apple, 2021; Google, 2021). Increases in the demand for country living are now rapidly taking place at least in the UK (Which, 2021). These trends are consistent with previous plagues and until herd immunity is reached through a combination of lockdowns, vaccinations, and control of global travel, the pandemic will continue to dictate how we move around and locate ourselves in cities. The percentage of persons working from home, the use of mass transit, and the control of shopping and social events have already varied dramatically with respect to successive waves of infection while many national and local economies have nose-dived in terms of their GDP. The extent to which they will bounce back once the pandemic comes under control is unclear. At the same time, the economy has been supported by the massive use of internet technologies which have enabled people to work, learn, and shop from home in ways that are completely unprecedented, and it appears likely that these forms of interaction will continue to be used in one form or another.

The biggest questions currently being posed involve the manner in which we will return to the old normal or develop a new in terms of where and how we live and work in cities. To an extent, the forces of centralisation and decentralisation in cities are usually balanced at any time but the massive disruption posed by the pandemic has resulted in completely artificial forms of such functioning that are impossible to reconcile with previous forces. As we release the lockdown, we need to speculate on how many people will continue to work from home, changing their preferences for travel, particularly on public transport, and truly engaging in the internet market place. Our abilities to predict such futures even before the pandemic began were not good and our previous models appear no longer relevant. Therefore to provide a framework for informed speculation, we will begin with a hypothetical model of a city system constructed geometrically and symmetrically around a city centre or core which we assume to be the origin of urban growth. We will build a model of movement and location for such a structure based on long-standing theories of spatial interaction (Wilson, 1971) and we will proceed to lockdown this structure, thence simulating a slow release towards a new normal. Our

quest is to explore the conditions under which the city might explode towards its edges as people relocate and travel further away from traditional workplaces, or implode as they flock back to its centre. We do not have any evidence of how resilient our existing city structures are to both a pandemic and the sea change in transportation technologies through the internet as well as the introduction of autonomous vehicles that are taking place in parallel. Thus the future is largely unknown but we consider a hypothetical model which we can then transfer to a real city an effective way forward.

We first introduce the model, lock it down according to different assumptions concerning working from home, and then slowly release the lockdown (over ten time intervals) until everyone is back at work in terms of the old normal. However as the lockdown is released, the locations of the most attractive places for work and residence also change and the new equilibrium that emerges is able to embrace a wide variety of different forms, from highly centralised to completely decentralised. This mirrors concentration in the core or on the periphery and all possibilities in-between. A key part of this exploration are variations in the travel preferences which are encoded in the spatial interaction functions that make different concentrations of employment and population possible. Having explored various hypothetical forms, we scale the model up to London and its region, introducing the intrinsic asymmetry and heterogeneity of the metropolis in terms of its massive business core, its various employment and retailing hubs, and its transport network. We then change travel patterns and preferences as we release the metropolis from lockdown, illustrating how travel patterns generate very different heterogeneities in future urban forms merging both radical and conservative ways of working and travelling.

The Hypothetical City

We define a city here as a set of N locations, $i, j = 1, 2, 3, \dots, N$, which form a square grid defined as an $n \; x \; n = N$ set of cells. We assume these cells are square, adjacent and contiguous to one another but the system can be easily relaxed to take on any 2-dimensional geometry that is appropriate. Each grid square i has a centroid defined by coordinates x_i, y_i and although the grid can be scaled to any size, we assume here that one of these zones is its geometric centre. To ensure this, n needs to be an odd number and here we set $n = 11$ with $n^2 = N = 121$ zones that we consider manageable for exploring and visualising this prototype. We begin by constructing a default pattern of movements defined as T_{ij} which measures the flows between all 121 zones where i defines the origin of the activity where people live and j defines the destination of the activity where people work. In this sense, T_{ij} is the 'journey to work'. We first simulate this using the most basic gravitational model based on the inverse square law of distance $T_{ij} \propto 1/d_{ij}^2$ where d_{ij} is the crow-fly or airline distance between origin zone i and destination zone j. We normalise this equation so that the total trips add to some predetermined total T writing the formal model as

$$T_{ij} = T \frac{A_j^{\alpha} d_{ij}^{\beta}}{\sum_i \sum_j A_j^{\alpha} d_{ij}^{\beta}} \qquad where \qquad \sum_i \sum_j T_{ij} = T \qquad . \qquad (1)$$

To derive the predicted numbers of residents at i called origin activity $O_i^{\&}$ and the number of workers at j called destination activity $D_j^{\&}$, we sum equation (1) over j and i respectively to get

$$\sum_j T_{ij} = O_i^{\&} \quad and \quad \sum_i T_{ij} = D_j^{\&} \quad . \tag{2}$$

It is immediately obvious that the system is symmetric if $d_{ij} = d_{ji}$ and then $T_{ij} = T_{ji}$. From the summations in equations (2), the origin and destination activity are equal – that is the same number of workers work in each location as the working population that lives there, that is $O_i^{\&} = D_i^{\&}$. This of course yields an entirely artificial situation never likely to be found in reality although various explorations have been conducted to explore how far real interactions within cities differ from symmetry (Tobler, 1976). In fact the gravitational force encapsulated in the inverse square model in equation (1) has been considered an effect that should be factored out before any simulation takes place because it is an artifact of the system's geometry (Coleman, 1964). Here we use this as a default geometry that we build on top of in the following manner. This default is illustrated in the grid in Figure 1(a) with the distribution of origins and destinations identical in Figure 1(b).

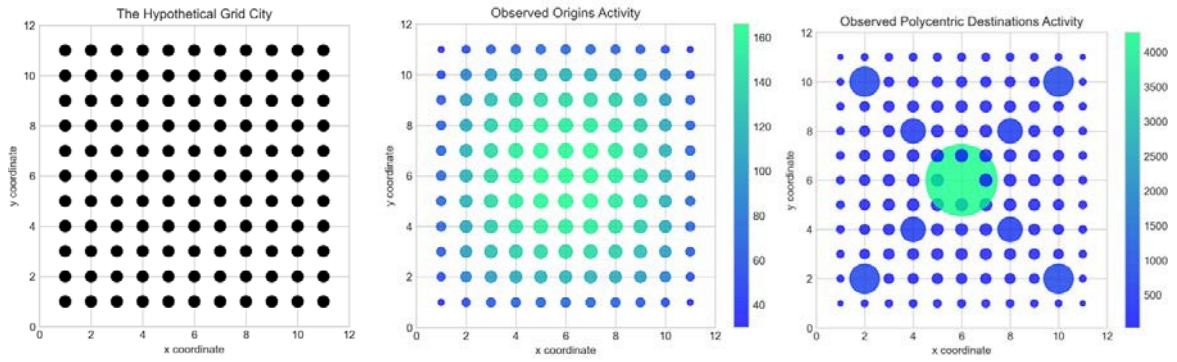

Figure 1: The Hypothetical Grid City

a) The 11 x 11 Grid b) The Observed Origins and Destinations by Size ($O_i^{\&} = D_j^{\&}$), and c) The Imposed Polycentric Hierarchy on the Destinations in b)

This default landscape is far from what we observe in real cities. Within such urban fields, a hierarchy of different sized centres is usual where the single major centre is by far the largest (Christaller, 1933). We thus impose a simple hierarchy of centres on this landscape by increasing the central destination D_{66} 5 times, doubling the size of the subcentres at $D_{36}, D_{63}, D_{93}, and\ D_{39}$, and trebling $D_{33}, D_{99}, D_{69}, and\ D_{96}$. We keep the origin distribution the same as in Figure 1(b) and we show the new destination distribution which contains the hierarchy of employment centres in Figure 1(c). This is the system we take as our starting point. It is not as peaked as a real city but its strong symmetry is almost impossible to break. This dominates all our subsequent explorations until we introduce some noise and move towards the real city in subsequent analysis.

We are now in a position to fill in the detail regarding travel patterns linking the origins and destinations in Figures 1(b) and 1(c) together using the standard doubly constrained model with a negative exponential function of distance. We state this as

$$T_{i\#} = A_i O_i B_\# D_0 \exp(-\beta d_{i\#}) \quad , \quad (3)$$

where O_i and $D_\#$ are the observed numbers of origins and destinations. The scaling constants A_i and $B_\#$ are chosen so that the model is consistent with these origin and destination constraints

$$\sum_\# T_{i\#} = O_i \text{ and. } \sum_i T_{i\#} = D_\# \quad , \quad (4)$$

while the constants also called competition terms or balancing factors A_i and $B_\#$ are solved iteratively. These are weights on the origins and destinations that ensure the trip matrix meets its constraints. The parameter β is closely related to the mean trip length which we define as $C = \sum_i \sum_\# T_{i\#} d_{i\#} / \sum_i \sum_\# T_{i\#}$. If we choose $\beta = 1/C$ which is 0.397, this generates a mean trip length for the model in equations (3) and (4) as $C = 3.388$. This would appear to be a reasonable value for a system with the dimensions of our default hypothetical city where the maximum distance across the system is 7.071 units. The system is still strongly symmetric although the flows now reflect the relatively flat distribution of origins and the relatively peaked hierarchy of destinations. Further details of the way the hypothetical system has been defined are included in the Supplementary Information (SI).

Imposing Lockdown, Simulating Its Release, and Diversifying the Urban Landscape

Once the pandemic began in earnest in March 2020, the rapid movement to working from home, the reduction in the use of public transport, and the slow but significant change in behaviours due to social distancing have all pushed people to live and work further from their traditional places of work. These elements can be introduced into our hypothetical city through changes to the functions of spatial interaction as well as arbitrary changes in where people live and work dictated by public regulations aimed at containing the pandemic. First, we will move people from work to home and then examine how the pattern of origins and destinations adjusts to these kinds of disturbance. We define the proportion of the population working in their usual places of work (destinations) as λ, $0 \leq \lambda \leq 1$, with the proportion of those living and working at home as $1 - \lambda$. In essence, there is no change in terms of where people live but in the different scenarios based on varying proportions of those working from home, workers are assigned from their job locations to their home locations according to the overall proportion $1 - \lambda$. We do not vary this proportion with respect to locations in the UK for we have no data although we know it varies for aggregates of key workers (see Farquharson, Rasul, and Sibieta, 2020). We assume however that this proportion is stable over all workers and locations in our toy city and from this, we are able to produce new scenarios based on a simple scaling and reallocation of jobs to home locations.

A new distribution of trips $\tilde{T}_{i\#}$ which differs from the original modelled distribution $T_{i\#}$ can be defined by simply assuming that $1 - \lambda$ of those living at home now work from home. All workers still live at the locations (origins) where they lived before the lockdown but $1 - \lambda$ not only live but now work from home. Formally those living at home can be defined $\tilde{O}_i = \lambda O_i + (1 - \lambda) O_i$ while those now working at their traditional places of work can be defined as $\tilde{D}_\# = \lambda D_\# + (1 - \lambda) O_\#$. All our lockdown scenarios are based on

changes to trips and destination activities $T_{i\#}$ and $D_{\#}$ that depend on the proportion $1-\lambda$. It is this parameter that we will vary from $\lambda = 0$ where everybody is working from home to $\lambda = 1$ where no one works from home, moving and locating according to the artificial polycentric city illustrated in Figure 1(c) and repeated in Figure 2(a) which is our starting point.

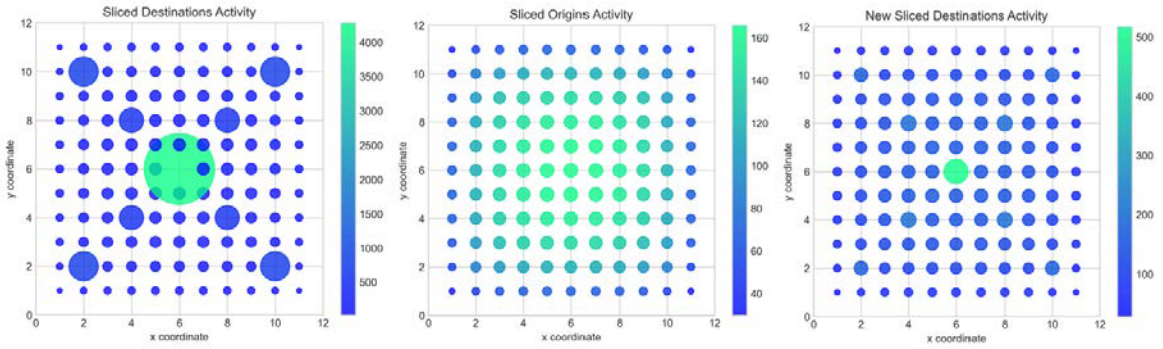

Figure 2: The Hypothetical Polycentric City with $1-\lambda = 0.8$ *Working From Home*

a) Polycentric Destination Locations D_j as in Figure 1(c) b) Origin Locations for Those Working from Home and Living at Home O_i c) Destination Locations for Those Working at Their Original Workplaces and Those Working from Home δ_j.

We have explored a range of possible regimes based on working from home which involve changing the distributions of workers at their place of work $D_{\#}$. The origin distribution remains the same as pictured in Figure 2(b) for any value of λ. As we increase λ from 0, the polycentric pattern of workplaces reveals itself and as λ approaches 1, the polycentric pattern in Figure 2(a) appears. We show the default where 80% work from home and 20% work traditionally in Figure 2(c).

There are many ways of measuring the differences in morphology which are occasioned by what we loosely refer to as slicing the workplace into those who work from home and those who remain in their traditional workplace location. When everyone works from home, the mean trip length C is the lowest it can be which is the smallest distance in a cell which is $\sqrt{2}/2$. As the proportion working from home decreases, this trip length increases back to the level defined in the original data $C = 3.388$. We will first explore changes associated with the lockdown based on the proportion $1-\lambda$ of the population working from home by assuming that the model linking origins to destinations in the polycentric city simulates a changed landscape based on these new numbers of persons working from home. In short we use a variant of the balanced interaction model in equation (3) to simulate a new and changed distribution of origins and destinations. This is based on the initial unchanged origins and the new destination distributions associated with the lockdown. We use these as inputs to an unconstrained gravitational model that recomputes the numbers of persons in origins and destinations, arguing that this is a simulation of an emergent structure in a situation where $1-\lambda$ people work from home. But when the lockdown is released and they consider returning to work, the pattern of where such work is likely to be and where they wish to live will be somewhat different from that prior to the pandemic and under lockdown. In short, we take the sliced origins and new sliced destinations in Figures 2(b) and 2(c) and use these as inputs to an unconstrained gravitational model which predicts new patterns of location and

interaction. The model we use is based on a variant of equation (3) which uses the balancing factors A_i and B_j as weights on the original origins O_i and the changed destinations $\tilde{D}_j = \lambda D_j + (1-\lambda)O_j$. The model is defined as

$$\tilde{T}_{ij} = KA_iO_iB_j[\lambda D_j + (1-\lambda)O_j]\exp(-\beta d_{ij}) \quad where \quad \sum_i \sum_j \tilde{T}_{ij} = T. \qquad (5)$$

K, the scaling constant, ensures the flows add to T. The model is then used to predict new origins $O_i^{\&} = \sum_j \tilde{T}_{ij}$ and destinations $D_j^{\&} = \sum_i \tilde{T}_{ij}$ with the full results shown in Figure 3.

The origin activity where the working population resides is more polarised than the original distribution while the polycentric form for destination activity slowly returns. In fact this shows that the centralising forces implicit in the urban structure we have adopted are extremely strong and this is revealed by the difference maps in Figures 3(c) and (f). Note these differences are absolute values where the inner zones for both origins and destinations show locations where predicted activity is greater than observed in contrast to the outer zones show where activity is less. To attempt to break symmetry, we have developed the same sort of simulation but this time we have introduced a very substantial amount of noise. What we have done is to scale origins O_i and lockdown destinations $\tilde{D}_j$ by $[1 \pm rand(\,)]$ and this enables activities to grow to up to double their size or reduce to almost zero. After this randomisation, the activities are rescaled to reflect the total activity T in the system. We have rerun the model in equation (5) for a first iteration and then five more using outputs from the unconstrained model on each iteration to provide inputs to the next. Five iterations give a good sense of the long term structural equilibrium which appears to be heading to a form with everything concentrated at the core. Figure 4 reveals the picture on the first and fifth iterations.

Our initial foray in exploring spatial heterogeneity in this model is based on making comparisons between trip patterns simulated by the model at sequential iterations. As the initial model is not in equilibrium due to the imposition of lockdown, with each adjustment towards the new equilibrium, the trip patterns change. We can extract the differences between successive trip patterns and use this as a measure of stability. But we will postpone this until later when we deal with more explicitly temporal variants of the basic model. In these early experiments, the degree of difference in interactions is in fact low for there is no evidence of symmetry breaking in the landscapes in Figures 3 and 4. In fact, this is quite the reverse with symmetry strengthening despite the high degree of noise we have imposed. We have run the model for many more iterations (>50) and what happens is that all the activity with respect to both origins and destinations ends up at the central zone. One very strong implication from this paper and from the model is that in any return to normality (which will be a new normal in any case), all the forces suggest that the city will not explode but return to its concentrated form. However, to explore how we might simulate a more diverse city, one in which it is easier to detect changes in the degree to which activities concentrate or disperse, we need to explore how we can change travel behaviour in the model and the city system.

Reconfiguring Travel Behaviours

So far we have hinted that changing behaviour in our hypothetical city through different measures of lockdown is not likely to be enough to generate radically different degrees

of concentration at the centre of the city than those that existed prior to the pandemic. What appears to be needed are opportunities to change the influence of distance on travel behaviour and this will involve changing the way populations locate with respect to home and work.

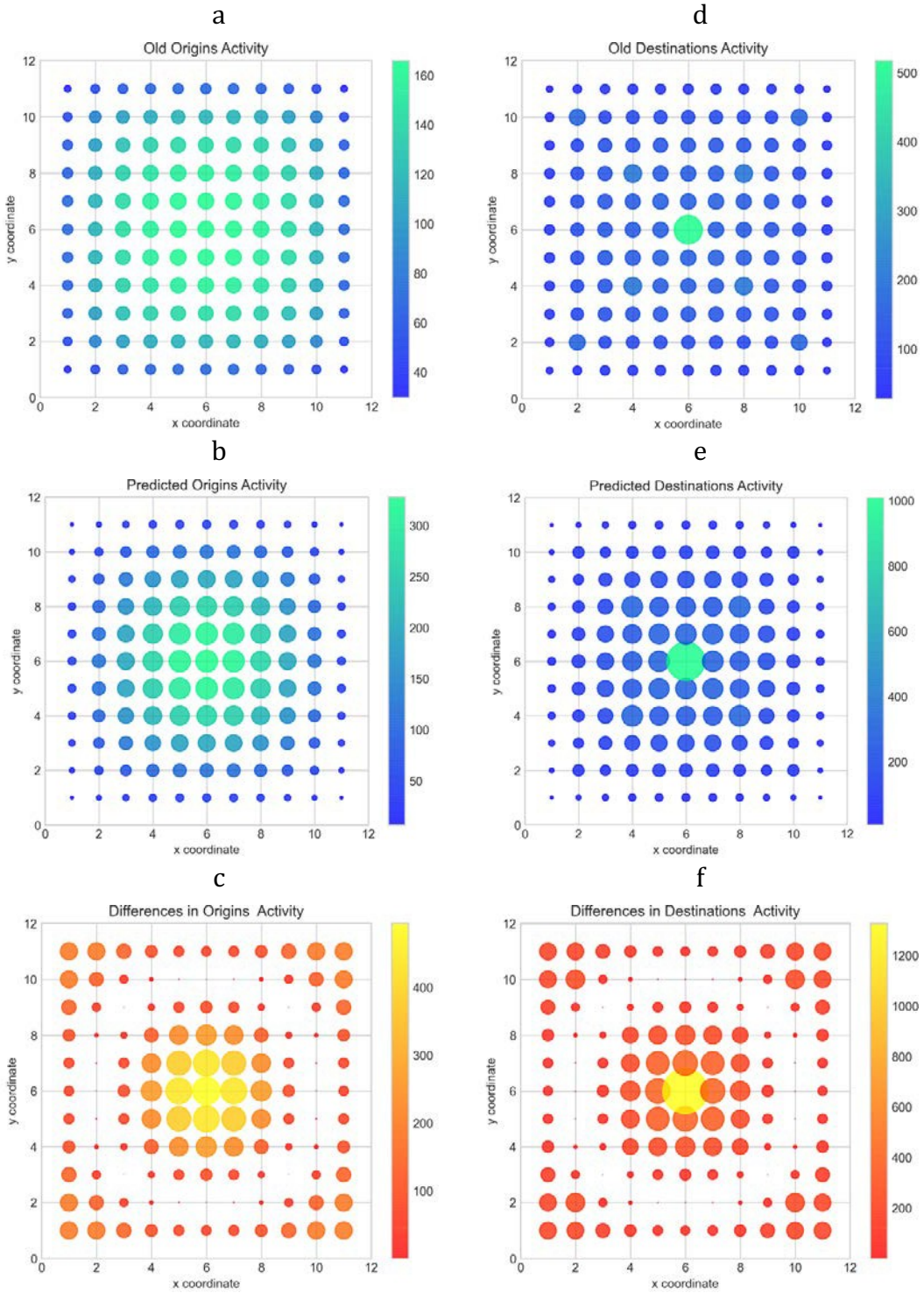

Figure 3: Simulations of Origins and Destinations Based on 0.8 *Working from Home*

a) Working at Home Origins b) Predicted Origins c) Scaled Differences based on $|O_{\%} - O^{1}_{\%}|$ d) Still at Work Destinations e) Predicted Work Destinations f) Scaled Differences based on $|D_{\cdot} - D^{\&}_{\cdot}|$,

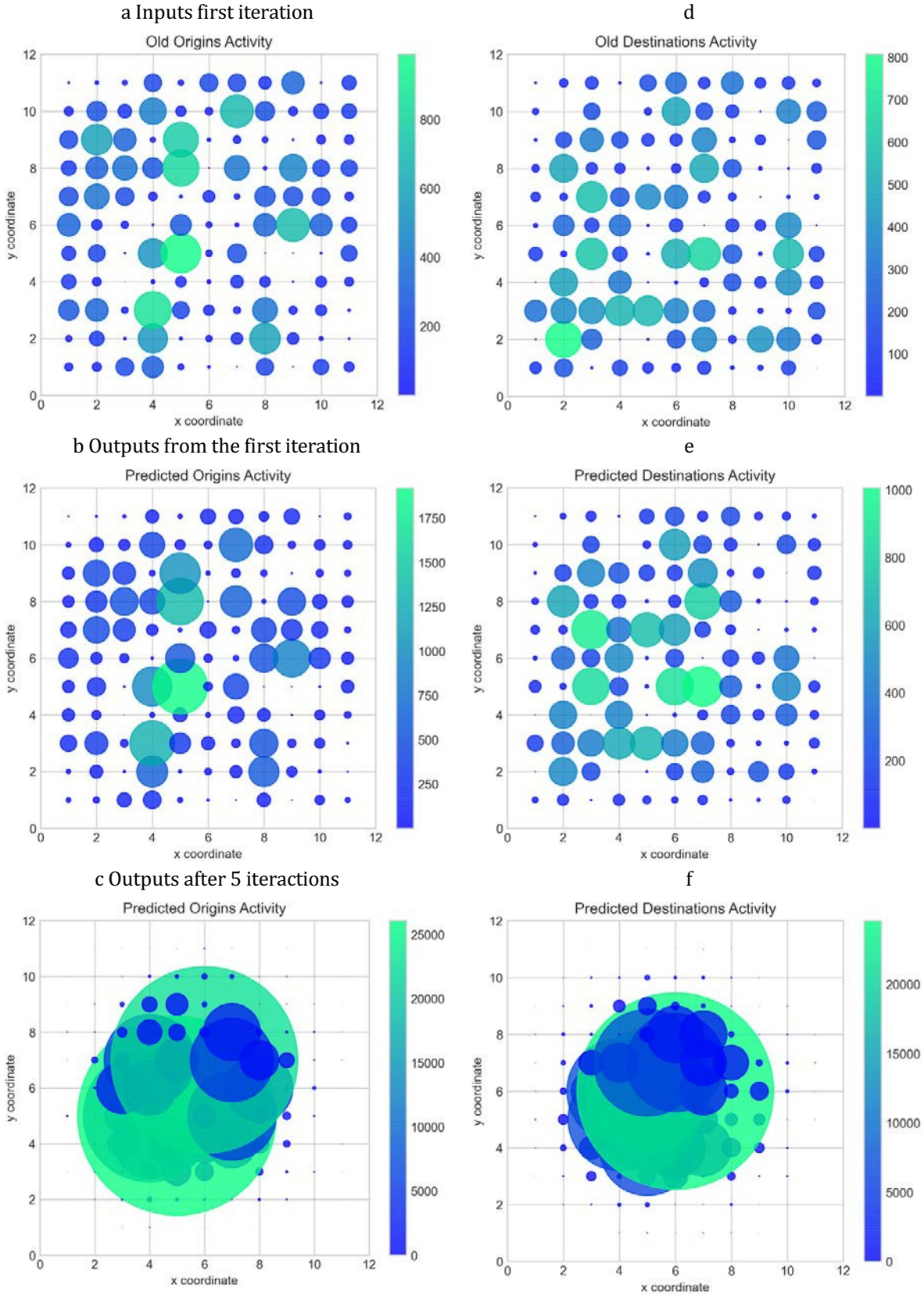

Figure 4: Solution of the Transition to Equilibrium in Five Iterations from the Randomised Lockdown of Origin and Destination Distributions of Residents and Workers

So far we have assumed that movement varies inversely with respect to the distance from some source (an origin or destination). This is the so-called 'First Law of Geography' or Tobler's Law (Tobler, 1970) and we first articulated this in constructing our hypothetical landscape based on the inverse square law $T_{ij} \propto d_{ij}^{-2}$. But once we layered the urban hierarchy on top of this, we used the more widely accepted negative exponential function $\exp(-\beta d_{ij})$ to generate a consistent pattern of movement as reflected in equations (3) and (4). In fact neither of these inverse distance functions is entirely suitable. The inverse square law is undefined at zero origins and predicts far too many interactions at small distances while the negative exponential function is unable to deal with movement at small distances where there are mild preferences to live some distance away from work.

We need a function with much greater flexibility that combines both inverse power and negative exponential effects. The function we adopt is

$$T_{ij} \propto d_{ij}^{\alpha-1} \exp(-\beta d_{ij}) \qquad (6)$$

which has gamma-like form where the parameters α and β control the friction of distance for the power and exponential functions respectively. When $\alpha = 1$, the power function collapses, the function reverting to the negative exponential. When $\beta = 0$, the negative exponential collapses and the model reverts to the power law. When $\alpha > 1$, the power law no longer acts as a deterrent effect but as an attractor but this is moderated by the negative exponential which acts as the deterrent. It was first proposed by Tanner (1961) to handle small distance effects in trip distribution models but in generalising the gravity model to embrace economic effects, it has been used several times since Tanner's original formulation (see Cochrane, 1975). In Figure 5, we show nine different variants, these being the functions used in the sample simulations that follow. In fact we illustrate these in detail in the SI and simply pick out the major characteristics of these simulations here in the main text. Note that the class of spatial interaction models we have defined is easy to extend to related discrete choice and even constrained non-linear regression models. These can be embedded in the same structures that we use here, but it is beyond the scope of this paper to develop these variants. Readers however need to be alerted to these possible extensions.

We have taken as our starting point the locked down city with 80% of the working population working from home as reflected in the baseline case shown in Figure 2. This baseline which is produced from the pure negative exponential distribution based on the unconstrained gravity model in equation (5) is Scenario 1 where $\alpha - 1 = 0$ and $\beta = 0.5$. When we lower β to 0 the pattern is less polarised and as we move to $\alpha - 1 = -1$ and $\beta = 0.8$, the pattern in the first Scenario begins to reassert itself. We then switch the parameters to $\alpha - 1 = 6$ and $\beta = 0.2$ and generate a city which is blown to its periphery with origins and destinations increasing inexorably from centre to edge. This is clearly generated by increases in $\alpha - 1$ which provides a distribution which acts in almost the opposite way from the inverse deterrence function. As we change $\alpha - 1$ and β to 4 and 0.6 and then to 2 and 1.0, the origins and destinations become less pronounced but begin to reinforce the traditional patterns focussed on the central zone. If we fix these at –2.5 and 0.2, we reinforce the monocentric pattern once again. If we then move to 6 and 0.4, we reinforce the edge effects and both origins and destinations decentralise. When we increase β to 1.0 and raise $\alpha - 1$ to 7, then the tension between these two elements in the

<)78+$:7 >$+9 +9" 6:>"3 52> 6)%9$7* +9" %;%+"= +: &"8"7+325$%" 27& +9" "G6:7"7+$25 +: 8"7+325$%"- 5"2&% +: 2 =:3" =)+"& 62++"37 %$=$523 +: +9" :3$*$725 5:8D&:>7 $7 M$*)3" K?

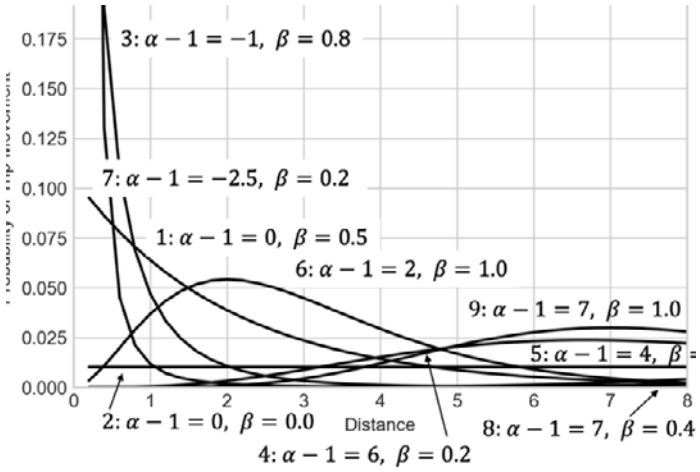

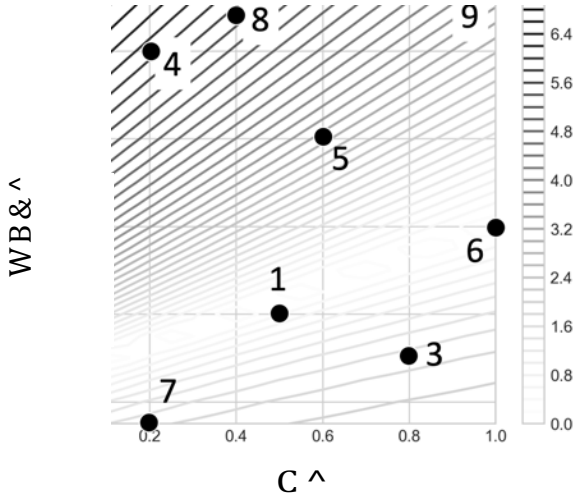

*"#$%&' M) N "2=#3- /A *&2I'3 8&/H2H#3#0- C#@0&#H%0#/9@*

!" >!*!<%4%*/ I2,* 3+EE%*%24 J5<-+2!4+52/ 5E 4$% #K5 >!*!<%4%*)!<<! 3+/4*+-C4+52 2 0 3 (.+ 49 2, -" L+2% 7:%2!*+5/ 7=!22+21 4$% >!*!<%4%* 7=!:% M//5:+!4%, K+4$ J5245C*/ 5E N%!2 #*!0%? 3+/4!2:%

H" >$55 $55)%+32+" +>: "G+3"=" "G2=65"% <3:= +9$% %2=65" :< I &$<<"3"7+ +32#"5 4"92#$:)3% $7 M$*)3" J 2% L8"723$:% J 27& , H" %9:> 255 I $7 +9"$3 "7+$3"+; $7 +9" LO <:3 +9" 327*" :< 6232="+"3% <3:= W B & % B' _` a 27& C % JGJ _` &GJ %9:>7 $7 M$*)3" N? F9" ="27 +3$6 5"7*+9 2%%:8$2+"& >$+9 C $7 +9" *2==2 &$%+3$4)+$:7- E% 8! 8# /!#2!#38! 8# /!# $783"2%"% =:3" :3 5"%% 5$7"235; >$+9 W B & 27& C? H" %9:> +9$% $7 =:3" &"+2$5 $7 +9" LO >9"3" >" 25%: $7+3:&)8" +9" 5:* ="27 +3$6 5"7*+9 E % 8! 8# /!#c`d 2!#38! 8# /!#)%)255; 2%%:8$2+"& >$+9 +9" 6232="+"3 W B &?

</&8.#*#28 *2 6'1 62/:&.

L: <23 4:+9 :)3 =:&"5 27& +9" 9;6:+9"+$825 *3$& 8$+; +: >9$89 $+ 92% 4""7 2665$"& 92#" <:8)%"& :7 9:> %628" 27& &$%+278" 28+ +: 6)55 27& 6)%9 >:3D$7* 6:6)52+$:7% 4"+>""7 +9" 6528"% >9"3" +9"; 5$#" 27& >9"3" +9"; >:3D? F9" %+3:7* %;=="+3; 27& +9" <:8)% :7 +9" *":="+3$8 8"7+3" >9$89 +9" %[]23" *3$& $=65$"% 28+ +: 6)55 28+$#$+; 2>2; <3:= +9" "&*"% :< +9" %;%+"= +:>23&% +9" 8"7+3" >9$89 =:%+ :< +9" #23$2+$:7% $7 +9" 6232="+"3% +92+ 8:7+3:5 +9" "<<"8+ :< &$%+278" %"3#" +: 3"$7<:38"? S75; >9"7 >" $7+3:&)8" &"+"33"78" <)78+$:7% 42%"& :7 +9" *2==2- &: >" =:#" 6:6)52+$:7% 2>2; <3:= +9"$3 :3$*$7%- *"7"32+$7* %;%+"=% +92+ 4"*$7 +: "G65:&" +:>23&% +9"$3 6"3$69"3$"%? 07 +9$% %"8+$:7- >" 4"*$7 2*2$7 >$+9 :)3 42%"5$7" >:3D$7* 6:6)52+$:7% , 6"38"7+ 4"5:> +9"$3)%)25 82628$+; 2+ >:3D6528" 5:82+$:7% 27& +9"7 "G65:3" +93"" #23$27+% :< +9$% 3"5"2%" <3:= 5:8D&:>7- 8:785)&$7* :)3 "G65:32+$:7 4; $7+3:&)8$7* &$#"3%$+; $7+: +9" %;%+"= +93:)*9 327&:=7"%% $7 5:82+$:7 27& %825$7* +: =)89 4$**"3 *3$& %;%+"=%?

M$3%+- >" >$55 "G2=$7" 9:> +9" >:3D$7* 6:6)52+$:7 2+ +9"$3 +32&$+$:725 6528"% :< >:3D 2&^)%+% +: 2 7"> 527&%826" : 3"%$&"7+$25 :3$*$7% 27& >:3D6528" &"%+$72+$:7%? , 6"38"7+

of workers continue to work from home but the remaining 20 percent respond to potential changes in their locations which define this new normal. Our second variant is to simulate the same transition but at each time step, an increasing proportion of workers return to their traditional place of work until all are working 'normally'. But in this process the landscape of origins and destinations changes too and an increasing proportion of those working normally respond to this by changing their residential and employment locations. This also generates a new normal but different from the old and different from the first variant where the numbers of persons working from home remains the same. Third, we will look at how the situation restores itself to no one working from home but this time with travel behaviour based on the gamma function continually changing to account for persons working and living much further away from one other. This is a scenario where travellers react to distance in an almost opposite way from that specified in Tobler's Law.

Scenario 6: $\alpha - 1 = 2, \beta = 1.0\,, C = 3.33, C^{\mathrm{b}} = 1.08$

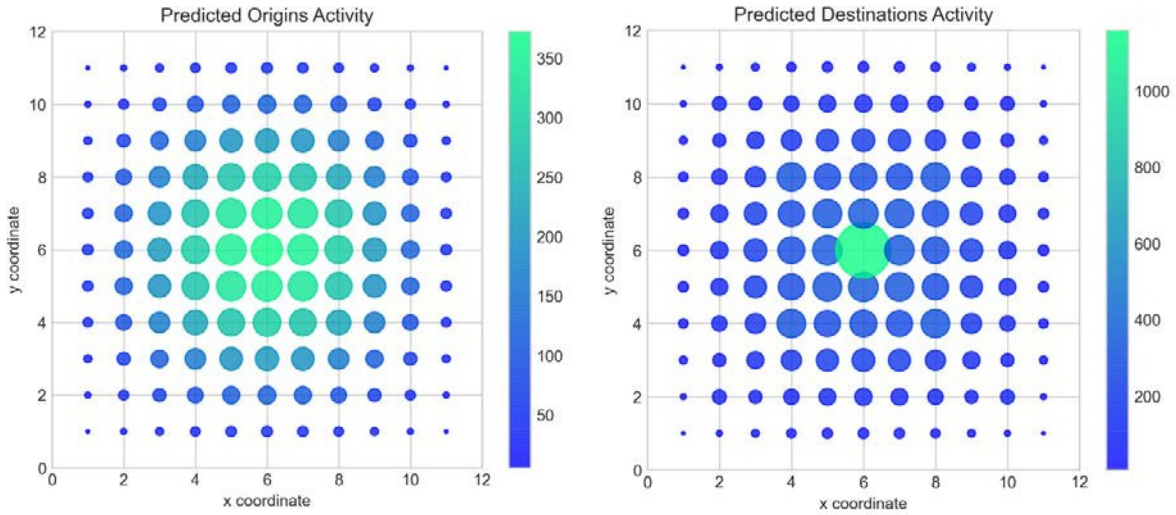

Scenario 8: $\alpha - 1 = 7, \beta = 0.4, C = 8.59, C^{\mathrm{b}} = 2.12$

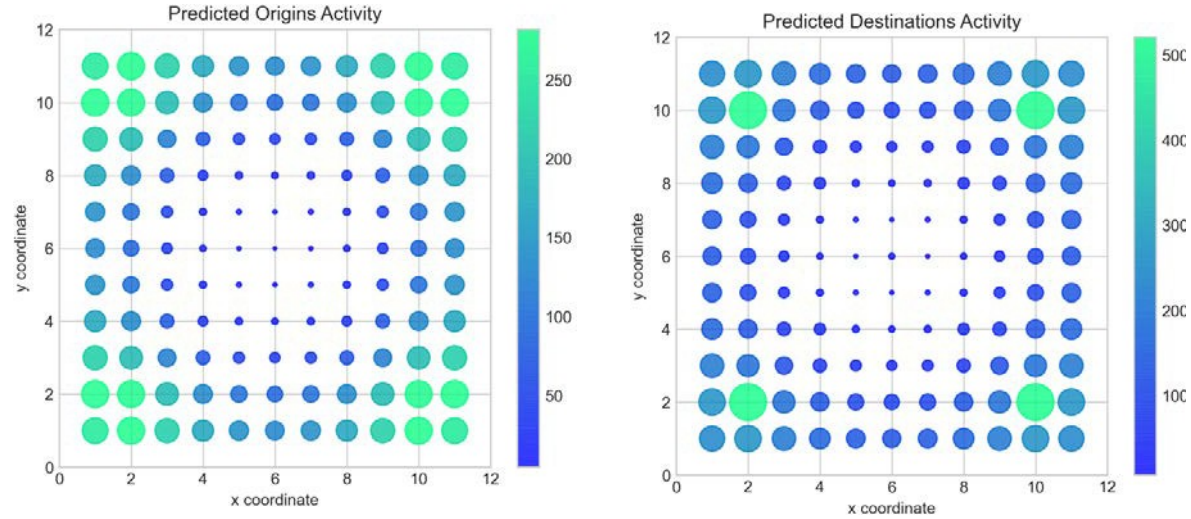

Figure 6: Scenarios 6 and 8 Showing Their Equilibria in Terms of Predicted Origins and Destinations Using Different Functions of Travel Behaviour

The model that we use to simulate the effects of workers who are not locked down and respond to the new gravitational landscape is based on equation (5). Origins and destinations associated with the number (λ) of non-locked down workers are defined as $O_i(1) = \lambda O_i + (1-\lambda)O_i$ and $D_j(1) = \lambda D_j + (1-\lambda)O_j$ and on successive iterations as $O_i(t+1) = \sum_j T_{ij}(t+1) + (1-\lambda)O_i$ and $D_j(t+1) = \sum_i T_{ij}(t+1) + (1-\lambda)O_j$. The model we use is

$$T_{ij}(t+1) = \lambda K(t) O_i(t) D_j(t) f(d_{ij}) \qquad where \quad \sum_i \sum_j T_{ij} = \lambda T \quad , \qquad (7)$$

which simulates the changing locations of those who have not changed their working habits during the pandemic but keeps those locked down, working from home, the same. We can do this for different proportions in the range $0 \leq \lambda \leq 1$ but we keep this fixed not at 0.2 which we consider an extreme lockdown but at 0.5 which we consider a more likely scenario which might persist after the pandemic is controlled. Continued substitution of the locational outputs $O_i(t)$ and $D_j(t)$ from equation (7) into its inputs leads to a sequence that we consider is likely to converge as we demonstrate in the applications below on our hypothetical grid. What we see when we examine this lock down is that as 50% of the activity is continually redistributed, the origin and destinations activities converge to unique patterns but they also appear to be converging on each other. In this limit, it appears that the pattern of work is identical to the pattern of residence as revealed in Figure 7.

As these models generate a sequence of different location and interaction patterns defined by $T_{ij}(t+1)$, $O_i(t)$, and $D_j(t)$, the differences between successive distributions computed as $\Delta T_{ij}(t+1) = T_{ij}(t+1) - T_{ij}(t)$, $\Delta O_i(t+1) = O_i(t+1) - O_i(t)$, and $\Delta D_j(t+1) = D_j(t+1) - D_j(t)$ provide measures of how similar these are from iteration to iteration. We can measure these differences for individual interactions i, j and locations i and j but more synoptic measures involve aggregations over all interactions and locations. We will simply define these for the change in total trip patterns each time period as $\mathcal{H}(t+1)$ and for the cumulative change $\mathcal{M}(t+1)$ from the first time period $t = 1$ as

$$\mathcal{H}(t+1) = \sum_i \sum_j |\Delta T_{ij}(t+1)| / 2T \text{ and} \qquad (8)$$

$$\mathcal{M}(t+1) = \sum_i \sum_j |T_{ij}(t+1) - T_{ij}(1)| / 2T. \qquad (9)$$

If the trip patterns are identical from iteration to iteration, this implies the system is in equilibrium with $\mathcal{H}(t+1) = 0, \forall t$ and $\mathcal{M}(t+1) = 0, \forall t$. This is equivalent to complete homogeneity between the trip patterns across time which we might consider to be a measure of zero heterogeneity. At the other end of the spectrum, the maximum value of these indices is unity which occurs when two successive trip patterns are entirely different. If the trip patterns are sufficiently different from one another on each iteration, then this is a measure of instability, or continuing heterogeneity. There are many variants on these measures and although it is not possible to engage in a complete discussion here, we will note them in our applications to London below.

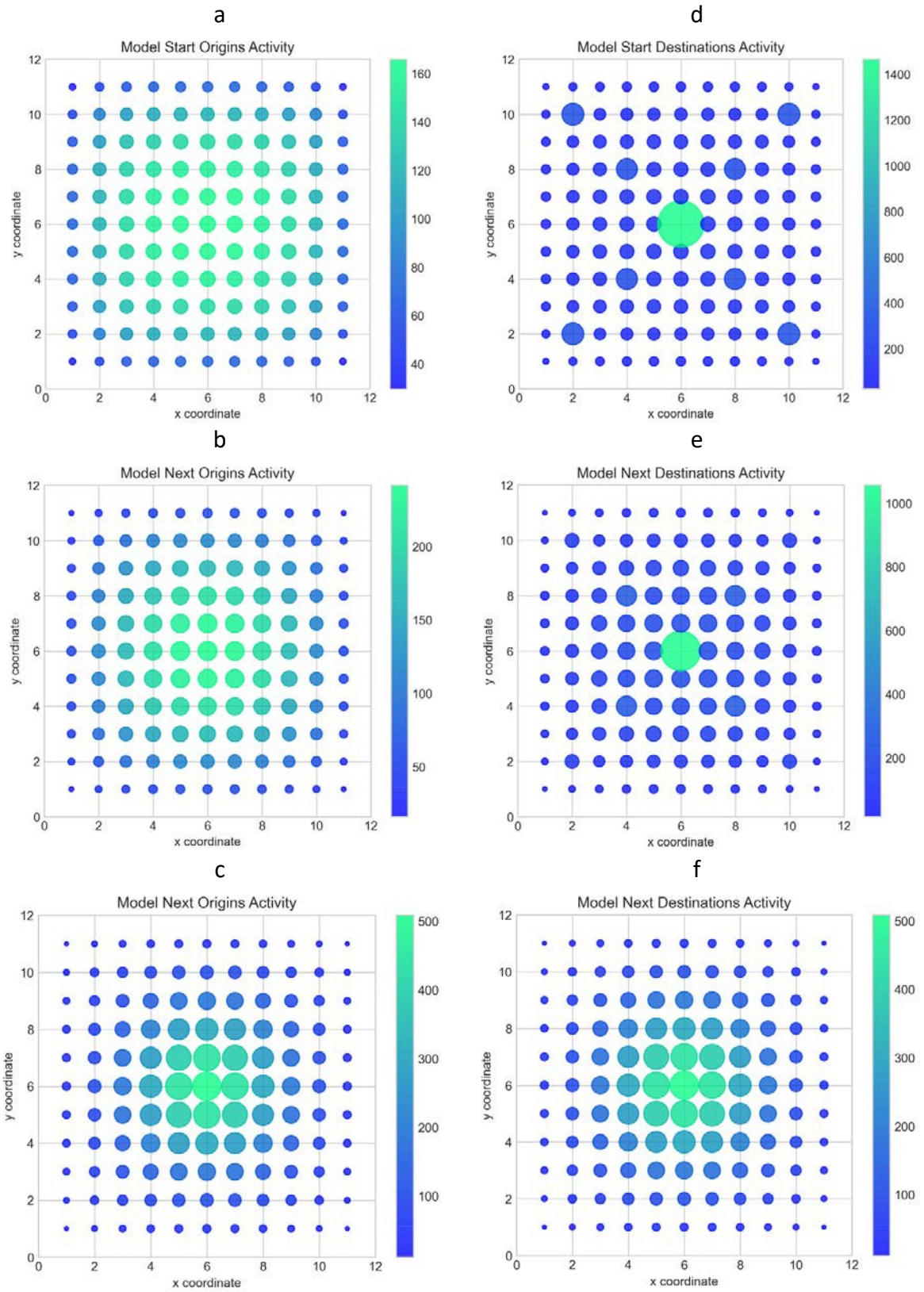

Figure 7: Transition to Long Term Equilibrium with $1 - \lambda = 0.5$ *Continuing to Work at Home*

a) Starting Origins *t=1* b) Second Origins *t=2* c) Long Term Origins *t=50* d) First Destinations *t=1* e) Second Destinations *t=2* f) Long Term Destinations *t=50*

Our second variant is based on a return to normality with the numbers of people working from home as 10% ($\lambda = 0.1$) through to everyone working traditionally (with none at

home). However as this transition takes place, the working population at workplaces (destinations) and residences (origins) continually readjusts to the changing landscape. We simulate this using the same unconstrained gravity model as in equation (7) above but with the temporal index now linked to the level of home working. We write the model as

$$T_{ij}(\lambda_{34}) = \lambda_{34} K(\lambda_{34}) O_i(\lambda_3) D_j(\lambda_3) f(d_{ij}) \qquad (10)$$

where λ_{34} is the proportion of population working at their traditional place of work. The transition from $0.1 \leq \lambda_{34} \leq 1.0$ can be as smooth as required and from this it is easy to make a movie showing how the centralising and decentralising forces act themselves out. In fact in the SI, we provide a glimpse of the key frames of such a movie at steps of 0.1 showing how the population moves back to full time working while at the same time centralising and converging on a longer term equilibrium which forces residential and workplace locations together. The measures of heterogeneity defined in equations (8) and (9) are generic in that they can be used with any set of trip distributions that change through time or through some iterative sequence. We can for example replace $T_{ij}(t+1)$ in equation (7) with the model in equation (10) based on $T_{ij}(\lambda_{34})$ and in the sequel, we can do this for each of the models presented.

From the model $\{T_{ij}(\lambda_{34})\}$, the solutions that we show in Figure 8 are theoretical possibilities but never likely to be manifest in this form. This however does provide a sense in which there can never be a transition back to normality for the way people will react is likely to be different from the way they have done prior to the pandemic. In fact, the 10-fold transition from $0.1 \leq \lambda \leq 1.0$ in steps of 0.1, along with the continual responses to the changed landscape of origins and destinations propels the city into a relatively concentrated form quite quickly, seemingly at a faster rate than when the percentage of persons working from home remains constant with rates of more than about 25%.

Our last substantive change is to introduce the gamma deterrence function that enables workers to locate at much further distances from one another than we currently observe. We illustrate this in the 9 scenarios configured in the previous section where we replaced the deterrence function with one combining power and exponential components into a form that balances attraction for living at greater distances away against the benefits of living nearer to any place. These functions are shown above in Figure 5 and in this section, we will choose one of these that first redistributes workers further away from the origin to a peak after which it subsides. This function is $d_{ij}^{b}\exp(-0.2d_{ij})$ and as in the other variants in this section, we run the model in equation (10) using the function in equation (6). This generates the following sequence where the density of activity at the outset has 80% of the population working at home, but redistributes itself continually, moving population towards the edge of the system. By the time everyone is back at work, the activity is largely located at the furthest distances from the centre of the grid, that is at the four corners of the square. Again, measures of heterogeneity can be computed but a detailed discussion is beyond the scope of this paper.

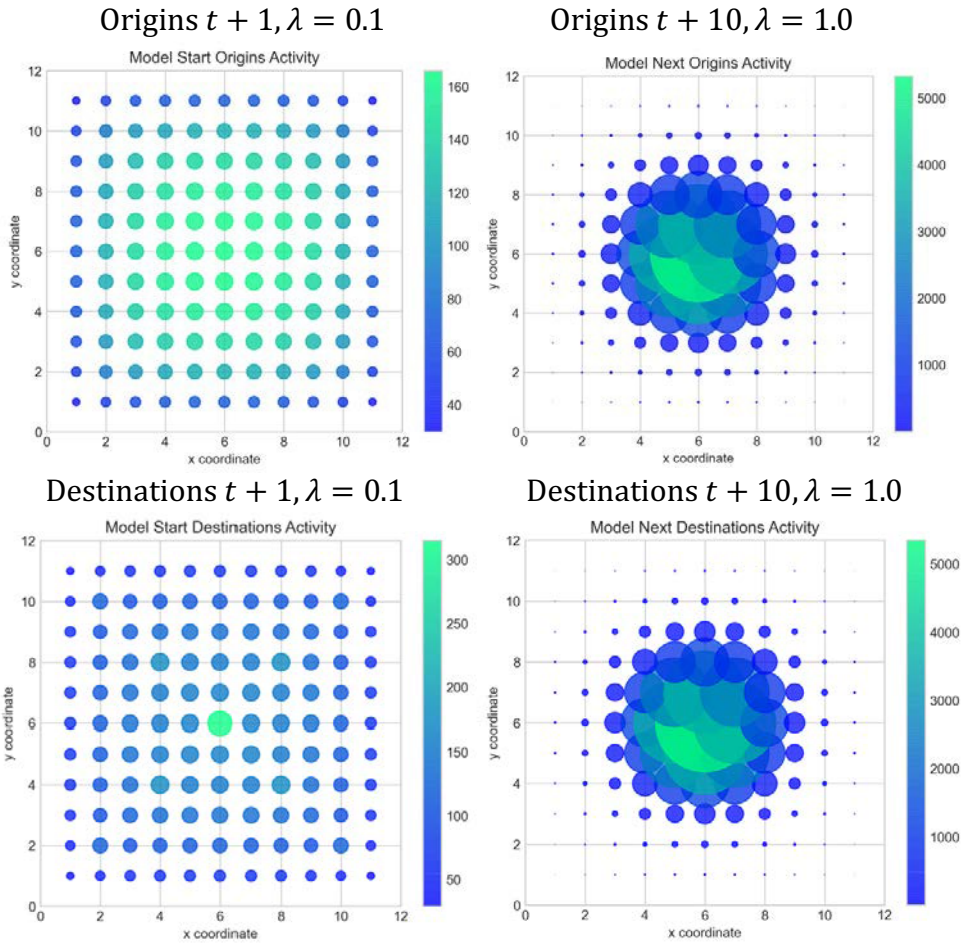

Figure 8: Transitions from Lockdown with 10% Working from Home Through to 100% Traditional Working

We show this in Figure 9 where it is clear that there are many ways in which we can redistribute activities reflecting the balance between centralisation and decentralisation. This balance of inward and outward forces also reveals some very complex issues for it is quite obvious that the development of a hypothetical grid system with the focus on its most accessible point at the centre and its least accessible at the four corners of the square grid provide limits when we come to develop this analysis for real cities. It might be argued that all that this effort has revealed are the major problems of space, density, deterrence, and boundary definition for applications involving how we travel and locate in cities but in doing so, we focus attention on the geometry of cities which has barely been explored to date other than in the most superficial terms.

The last thing we will do is to introduce a degree of randomness into this picture just as we did in an earlier section where we modified the origins and destinations using a random switch with an average of a $\pm 25\%$ difference from the basic input data. We do the same for the model in equations (10) where we also use the gamma function and the continuing release from lockdown. This alongside the introduction of a degree of randomness at each iteration which takes place over 10 time periods from $0.1 \leq \lambda_{34(} \leq 1.0$ in steps of 0.1, adds further to the heterogeneity of different locations of working population. The most surprising feature from this model involves the convergence to what appears a relatively stable solution for both origin and destination distributions while it appears that not only do these distributions converge but they also converge on

each other. These simulations are shown in Figure 10. We have scaled these up to systems with the dimensions of London which we will deal with next, showing these hypothetical simulations in the SI.

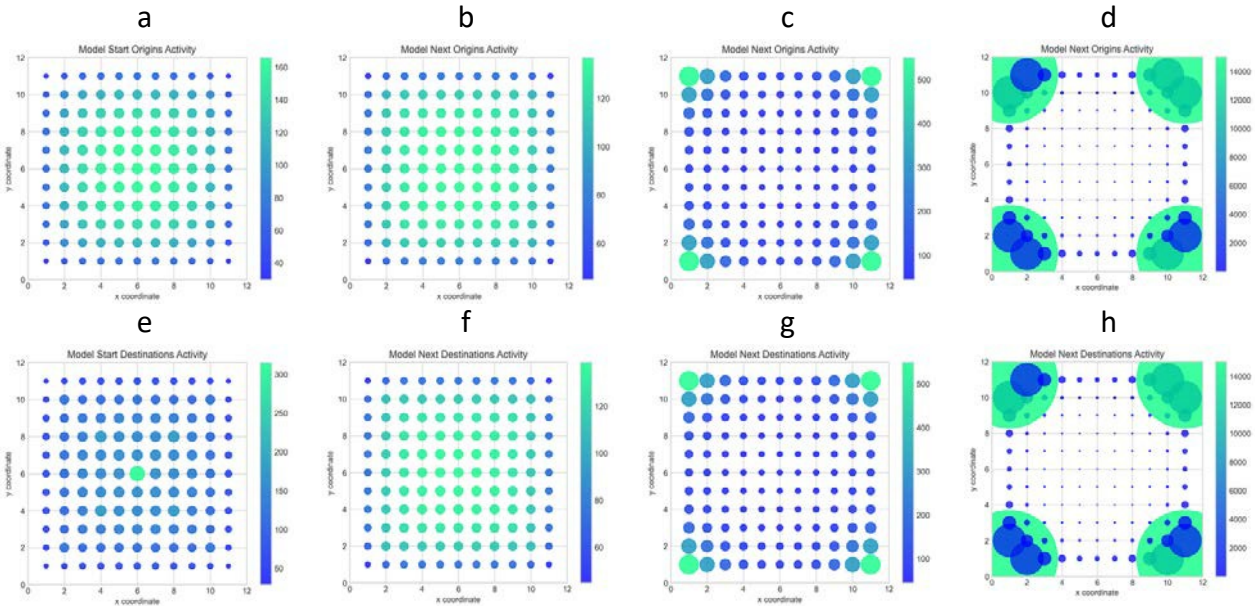

Figure 9: A Switch in Travel Behaviour: Scenario 4: α-1=6, β=0.2, using the Gamma Function $\sim d_{i\#}^{\cdot} \exp(-0.2 d_{i\#})$

Origin Activities a) t=1 b) t=2 c) t=5 d) t=10: Destination Activities e) t=1 f) t=2 g) t=5 h) t=10

A Kind of Realism: Applications to London

To proceed, we need to rehearse our argument: first, we will never have the requisite theory and technology to explain and forecast the future form of cities for they are complex systems that defy prediction; and second, that in the case of the pandemic, cities have been disrupted in ways that destroy much of the semblance of their previous order and make it impossible to know how they will return to a new normal. All we can do is engage in informed speculation, building plausible hypotheses which we proceed to test using simulation. In fact, there are few explorations of idealised urban futures using computer models (but see Tobler, 1970; Cecchini and Viola, 1990; and more recently, Schindler and Caruso, 2020). However, we now have robust enough technologies to do so. In what follows, we outline the application of the hypothetical model to London, first presenting its calibration to basic data for the last UK Census year 2011, updated to 2018. We show the distribution of population at origins where workers reside and at destinations where they work, noting the distinction between those who work at home and essential workers who continue to work at their usual workplaces. We define a solution space of possible future urban forms based on the three parameters defined above which control the percentage lockdown (λ), the attraction of living at greater distances from work (α), and the deterrent effects (β) of living further away from any

location. We identify seven scenarios which illustrate how the city can implode or explode under different sets of these parameters.

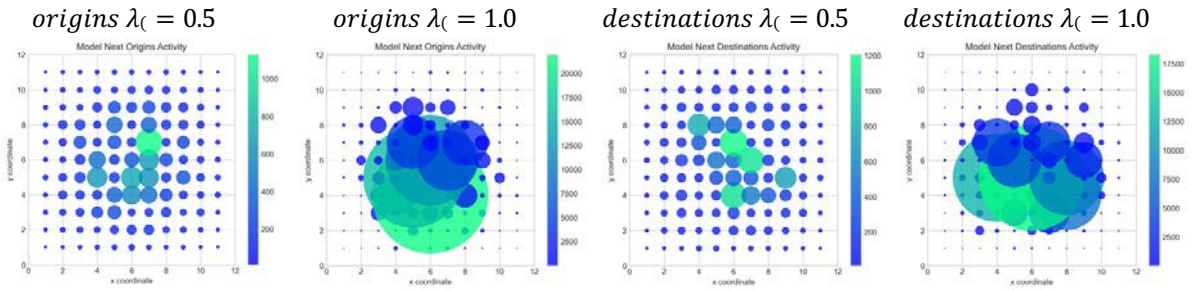

Figure 10: Introducing Randomness and the Longer Term Equilibria

The London metropolitan region is composed of some 1767 zones, small areas called 'wards' close to the UK Census geography of Middle layer Super Output Areas (MSOAs). The total population at origins is 13.43m and employment at destinations 6.83m with the average population of each zone 7599 and employment 3863. However these distributions are very highly skewed with the employment distribution having a coefficient of skewness of 12.099, more than 40 times greater than the population which has a value of 0.273. The correlation between these two spatial distributions (employment and population) is also quite low at 0.139. The dimensions of the spatial system defined by its bounding box are 80.228 miles by 72.467 miles where the maximum distance between zone centroids is 82.132 miles. We show the locations of the zone centroids in Figure 11(a) and the directional vectors with respect to the dominant trip orientations in Figure 11(b). It is quite clear that the symmetry of the system around the centre is still strong although its polycentric nature is obvious too with respect to towns that have been absorbed into the metropolitan area as it has grown. On the extreme west, we can identify Reading and on the east, Southend on the estuary. Key hubs Wembley, Heathrow, and Docklands – London's second CBD at Canary Wharf – stand out together with Watford, St. Albans and other suburban towns.

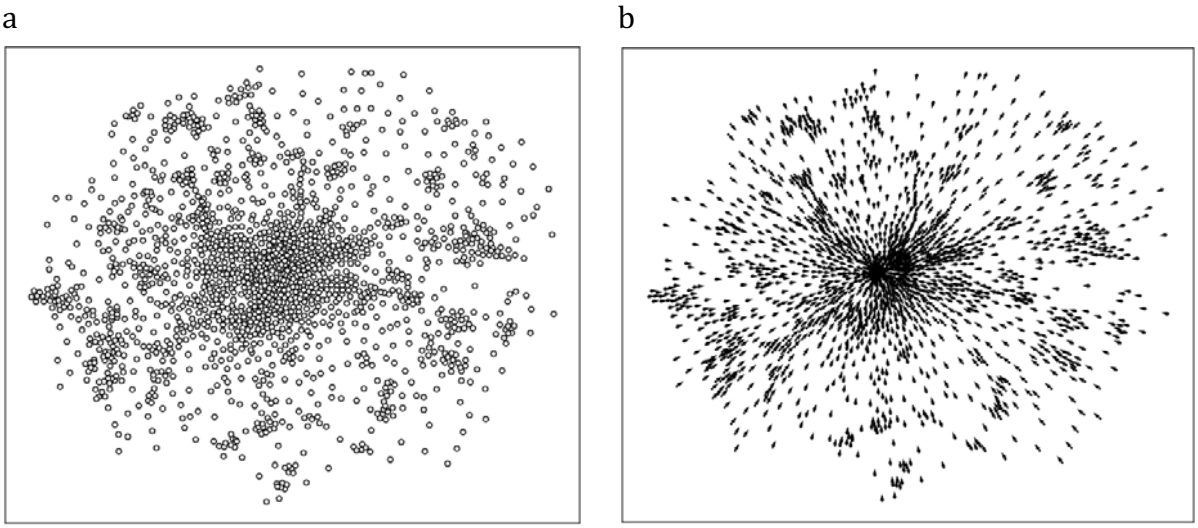

Figure 11: The London Metropolitan Region Data

a) Zone Centroids Based on Wards b) Vector Flow Directions Based on Trips from Residences to Workplaces

We scale the population at zonal origins i, O_i to the working population which sums to total employment at zonal destinations j, D_j, that is $\sum_i \sum_j T_{ij} = \sum_i O_i = \sum_j D_j = T$. We first calibrate a model of these flows using variants of the doubly constrained spatial interaction defined above in equations (3) and (4), but with interaction represented by the gamma-like function in equation (6) as $f(d_{ij}) = d_{ij}^{\alpha-1}\exp(-\beta d_{ij})$. We show these origins and destinations in Figures 12(a) and 12(b) respectively and we examine the skewness in the SI.

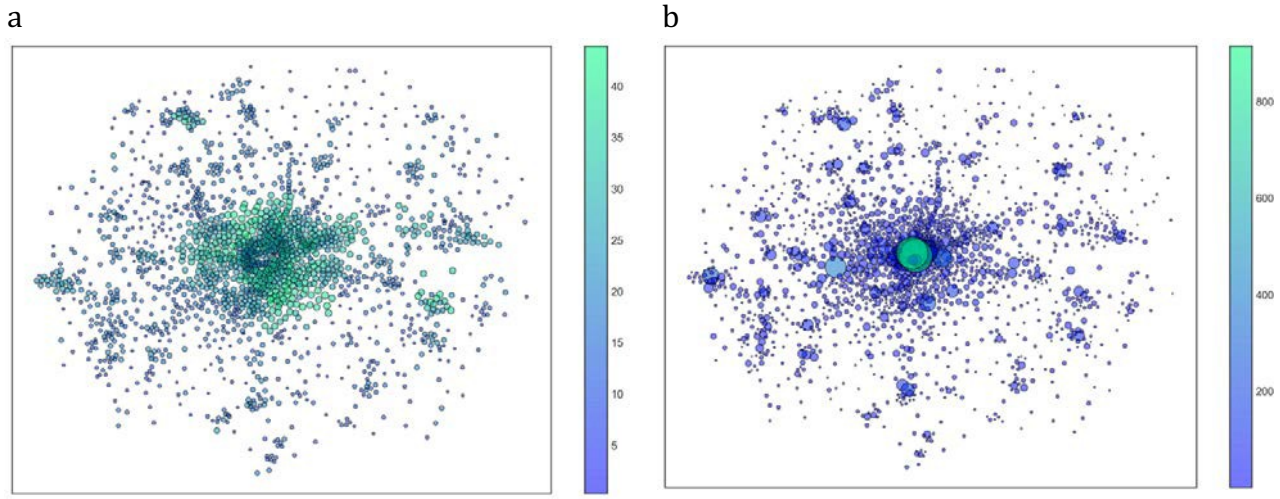

Figure 12: Population and Employment in the London Region

Population at Residences (Origins) of the Journey to Work Trips O_i b) Employment at Workplaces (Destinations) for Journey to Work Trips D_j

We calibrate the model in equation (6) assuming that the gamma parameter $\alpha = 1$, which implies that the attractor has no effect. We then choose the parameter β so that the predicted mean trip length $\bar{C}$ is equal to the observed mean $\bar{C}^{567}$. The observed mean $\bar{C}^{567} = 11.514$ miles with the value of $\beta = 0.094$ which we will round up to 0.1 We create the lockdown assuming a baseline with the proportion of persons working from home as $1 - \lambda = 0.8$, those who continue to work at their traditional workplaces $\lambda = 0.2$, and the proportion of persons making trips as λT_{ij}. In the SI, we map these new origins (which in fact are the original data) based on $O_i = \lambda O_i + (1-\lambda)O_i$ and the new destinations as $D_j = \lambda D_j + (1-\lambda)O_j$.

We will explore seven scenarios for London based on different combinations of the three key parameters λ, α, and β. We start from the simple baseline we call Scenario 1 where 90 percent of the population are working from home, that is, $1 - \lambda = 0.9$ and slowly relax this lockdown until only 10 percent work from home. For the first 10 time intervals, more and more of the working population and their households become footloose in that they change their workplace and residential locations as the overall level of lockdown falls to what we consider the most likely proportion of those working from home $1 - \lambda = 0.1$. We continue the simulation for another 20 time periods, and once this limit is reached, we consider the model has converged to a new normal beyond which there is little further change. During the entire period based on $t = 30$ time steps, the travel behaviour is kept at the default level with the gamma collapsed to the standard negative exponential function of deterrence where $\beta = 0.1$ and $\alpha - 1 = 0$ using the model $T_{ij}(\lambda_{34}) =$

$\lambda_{34(}K(\lambda_{34(})\hat{O}_!(\lambda_3)\hat{D}_\#(\lambda_3)d_{!\#}^{2(9))1(}$ expU$-\beta(\lambda_3)d_{!\#}$V based on equation (10). The assumed equilibrium after 30 iterations is not calibrated as we have no data pertaining to the speed at which people adjust to the changed distribution of employment and population.

There are a number of statistics we will compute for each scenario. We start with the mean trip length C and define four measures of how employment and population are related spatially. At any time t, we measure the coincidence between the origin activity and destination activity from

$$\Psi(\lambda_3) = \sum_!|\hat{O}_!(\lambda_3) - \hat{D}_!(\lambda_3)| \quad , \tag{9}$$

where this measure is zero if the two distributions are the same. We also speculate that if all the employment is in one place and all the population in another, then this measure would be at a maximum of $2T$. Other simple measures are the correlations between the initial pandemic origin and destination activities, and then between the predicted activities $O_!$ and $\hat{O}_!(\lambda_3)$, and $D_\#$ and $\hat{D}_\#(\lambda_3)$. Lastly, we measure the relative spread of the origin activity from the city centre where a large proportion of the activity is initially located. This is a measure of weighted distance

$$\phi: = \sum_! \hat{O}_!(\lambda_3)d_{!,(""}/N \quad , \tag{10}$$

where $d_{!,(""}$ is the distance from any origin zone i to a central zone (in the case of London, the Holborn-Covent Garden ward, zone [122]). If everybody lived there, this measure would be a minimum while if everybody lived at a maximum distance from this zone, the measure would be at a maximum. As such, this is a crude measure of suburbanisation.

In all seven scenarios, we keep $\beta = 0.1$ and vary the impact of the distance attractor $\alpha - 1$. Our baseline Scenario 1 negates the distance attractor by setting $\alpha - 1 = 0$ and in all scenarios, the lockdown is completely released from the original default during the first 10 iterations once $\lambda_/$ reaches 0.9. In the remaining 20 iterations, a long term equilibrium where the city implodes is generated as illustrated in Figures 13(a) and 13(b).

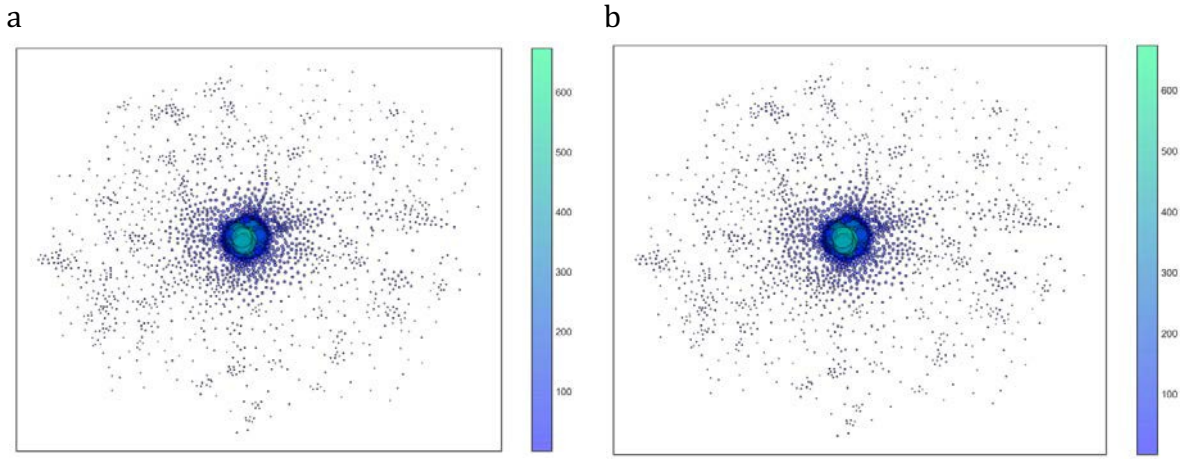

Figure 13: Scenario 1: Transforming the Old Normal Through Returning to Work and Restoring Relocation with $\beta = 0.1$ and $\alpha - 1 = 0$.
a) Origins, then b) Destinations after 30 Iterations which converge on one another

Comparing Figure 13 with the original lockdown, it is clear that starting with $\lambda_{(} = 0.1$ as the lockdown comes off, the trip length falls systematically to around 4 miles. The morphology concentrates dramatically, almost imploding in on itself where the individual zone centroids become denuded of activity as this all flows to the traditional and geometric centre of the city. We show the statistics for all seven of our scenarios in Figure 14. In fact, in the first scenario, the difference measure $\Psi(\lambda_3)$ converges but then begins to diverge although the differences are relatively small. When we look at the correlations $r\{O_!, \phi_!(\lambda_3)\}$, these get progressively smaller with respect to the original distribution but they do stabilise at around 0.25. The destination correlations $r\{D_\#, D_\#(\lambda_3)\}$ decrease slightly at first and then increase as the new normal destination activity is restored to its more traditional pattern with the employment distribution becoming closer to the initial distribution. The last measure of suburbanisation $\phi_:$ systematically gets smaller and this indicates that the city is becoming ever more concentrated in terms of employment. We use $\phi_:$ as an index of suburbanisation and in the default case this varies from a baseline of about 59409 to the compact city form where it reduces to 19480.

The second scenario is based on increasing the value of $\alpha - 1$ from 0 to 5 keeping β at 0.1. This systematically pushes people away from their workplaces generating strong suburbanisation with both origin and destination activities moving from centre to periphery. The mean trip length increases quite rapidly as more people come out of lockdown and revert to traditional work patterns and as the attraction of living farther from work continues to increase to a mean distance of more than 40 miles. This as one might expect, pushes both employment and population to the periphery of the system. When the old normal with respect to work has been restored after some ten time periods, although activity continues to decentralise, the pattern does not change much more as the new equilibrium emerges. We show the distributions at $t = 30$ in Figure 15. The suburban pattern becomes established quite early in the process with the $\phi_:$ measure doubling from some 59830 to 103373 while the correlations between origins and between destinations completely disappear by the time the final pattern emerges.

As activity is attracted from the core to the periphery, it tends to cluster in the bigger locations such as Reading, Southend, the Heathrow sprawl, Watford and similar edge-city like locations. Scenario 3 also changes travel behaviour but in the opposite direction to that introduced in the previous scenario. We assume that populations change their behaviour during lockdown to the point where they first wish to live far from their traditional workplaces. We start the sequence at $t = 1$ with a strong attraction to living further away and as the lockdown comes off, this effect through the gamma function reduces to the point where this function has no effect; that is, $\alpha - 1$ goes from 5 to 0 keeping β at 0.1 as before. The pattern that is revealed (which we show in the SI) does not differ markedly from the baseline. The average trip length is now 33 miles at the start, and this reduces to 4 miles when $t = 30$. The correlations have the same pattern as in the baseline while $\Psi(\lambda_3)$ falls dramatically as the employment and population patterns cluster very tightly. The index of suburbanisation also falls from 62919 to 20068 with the implication that in the steady state there is likely to be complete convergence on the centre for both population and employment. We also strengthened the attractor effect of the gamma function by increasing the parameter α to 5 for the duration of the simulation and the statistics are shown in the graphs in Figure 14 as Scenario 4. Scenario 5 keeps $\alpha - 1$ constant, reflecting a one-off transition from the pre-pandemic travel pattern to a new normal based on a distinct aversion to living near one another. We assume that the

gamma parameter is set at a value of $\alpha(\lambda_3) - 1 = 5, \forall t$ and the decentralisation in this scenario reveals that the mean trip length adjusts almost immediately to 30 miles and eventually converges to a very stable value of 44 miles. The suburban index ϕ: also increases from 63115 to 103927 which is extremely stable as the relevant trajectories in Figure 14 indicate. We show Scenarios 3, 4 and 5 in the SI.

a

Scenario No	β	$\alpha - 1$
1	0.1	0
2	0.1	$0 \rightarrow 5$
3	0.1	$5 \rightarrow 0$
4	0.1	$1 \rightarrow 5$
5	0.1	5
6	0.1	$1 \rightarrow -5$
7	0.05	$0.5 \rightarrow 5$

b

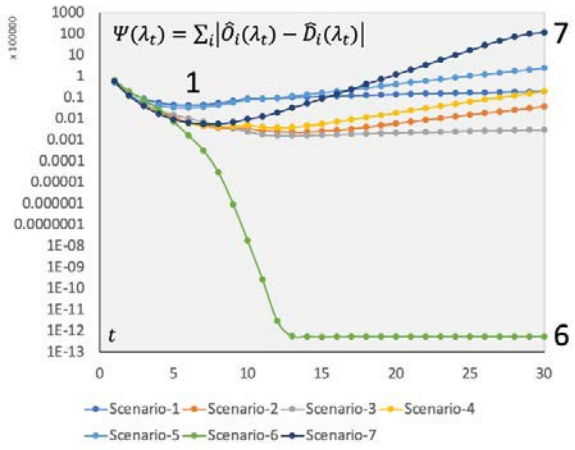

c

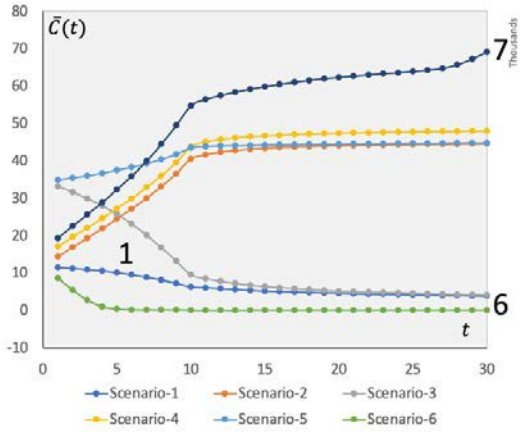

d

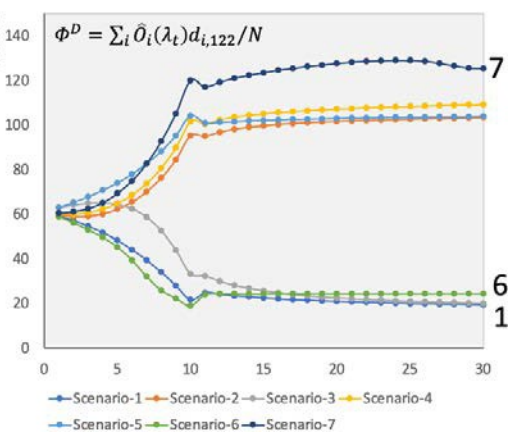

e

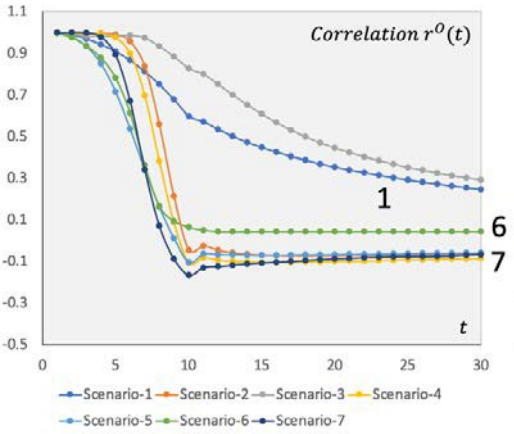

f

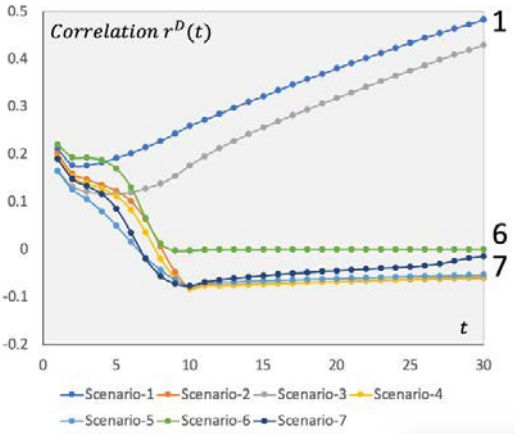

Figure 14: Statistics of the Transitions Back to Working in Traditional Workplaces and Continued Responses to the Redistribution of Residential Locations and Workplaces

a b

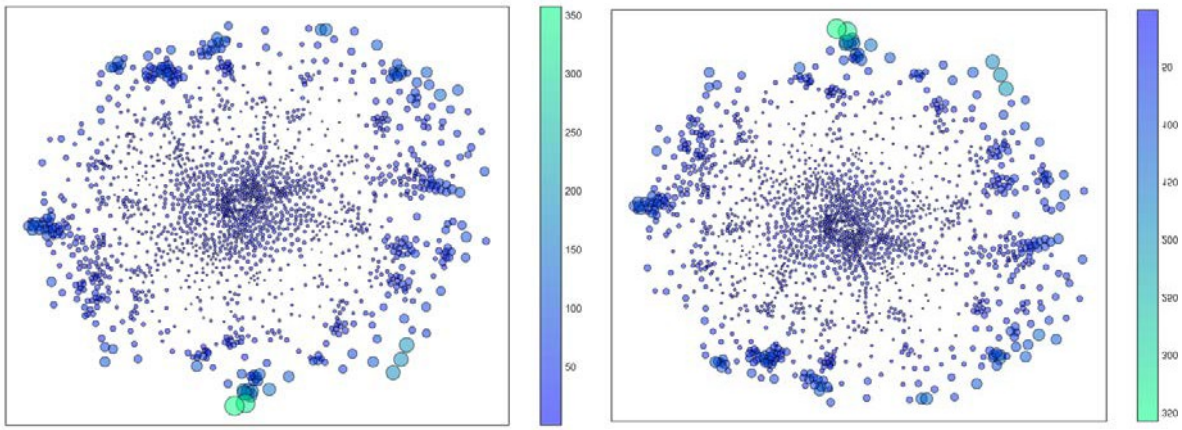

Figure 15: Scenario 2: Reducing the Deterrent Effect of Distance Using the Gamma Function

a) Origins, then b) Destinations after 30 Iterations

To conclude our brief discussion of heterogeneity in trip patterns that emerge as the working population evolves to a new normal, we will measure these differences between each iteration using equation (8) and the difference between the current iteration and the starting point using equation (9). We will do this for each of the seven scenarios defined above as illustrated in Figure 14. The differences at the start of the iterative sequence are about 20% and then drop quite rapidly to stabilise as the normal is approached for each scenario where it is clear the trip patterns between iterations become much more homogeneous. For the cumulative differences from the starting position, for scenario 6 this changes dramatically at the start as the parameters for this scenario represent a massive shift in travel patterns which are more than 95% different from the starting point whereas all the other scenarios increase linearly to end between 25% and 40% different from the starting point at the equilibrium. We show these graphs in the SI.

We will conclude by showing two more extreme scenarios. What we have done is reverse the effect of the gamma attractor by specifying a negative parameter value $\alpha(\lambda_3) - 1 < 1$ which we set at -5 . Almost immediately even before the population returns to its traditional workplaces, the mean trip length collapses as people essentially abandon any long distance travel. By the end of the lockdown, people have adjusted their work journey patterns to reflect a very close home-work balance. The system compacts itself dramatically with people essentially living and working in the same place as we show in Figure 16. We now show almost the reverse or opposite situation where we halve the value of the β parameter and increase $\alpha - 1$ to 5. This reflects the increasing attractor on distance, and it also lowers the impact of the deterrence effects, thus embodying a double impact on pushing population and employment at increasing distances from one another other. The mean trip length varies from 19.350 to 69.150 miles and this produces an extreme pattern where the majority of the population at origins live on the east and north east of the metropolis while employment is strongly clustered in the Reading-Heathrow area in the west. The model pushes all the population to locations on the east and all the employment to locations on the west, the most extreme kind of suburbanisation that is possible where residences and jobs are as separated as they can be.

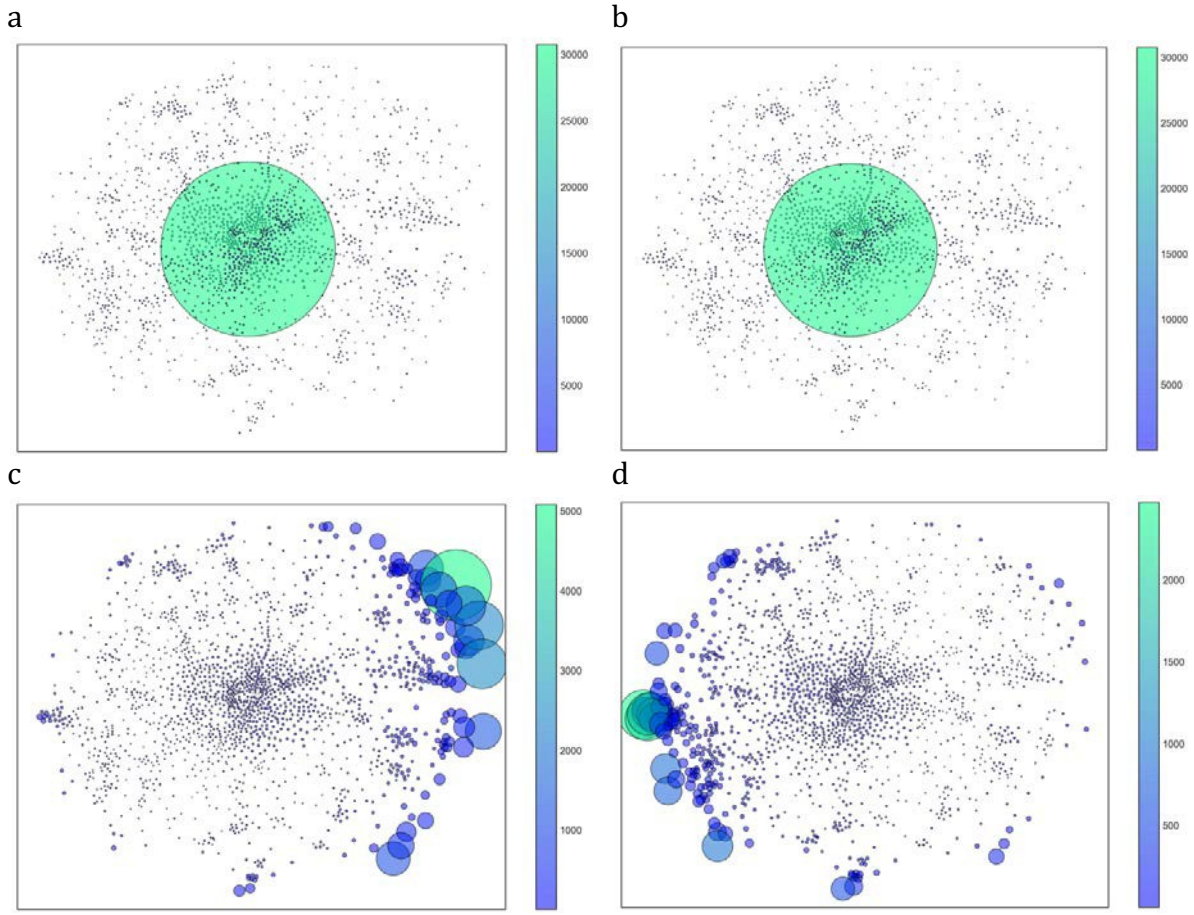

Figure 16: Extreme Scenarios: Increasing and Decreasing Resistance to Locating at a Distance Between Home and Work

a) Origins, then b) Destinations for Scenario 6; c) Origins, then d) Destinations for Scenario 7

Conclusions: Further Experimentation

We have only just begun to develop this approach to generating computable thought experiments and there is much else to do in combining plausible assumptions with speculative hypotheses. We have found it hard to break the symmetry of the monocentric city which is reinforced to an extent by the hierarchy of lower order centres. In the SI, we show that some scenarios are able to break symmetry but overall it appears that in moving to a new normal, returning to the central city is the most likely morphology for the post-pandemic city. There are many obvious extensions that need to be made to both the original hypothetical city and model and to its application to a large city, but many of these relate to how we might use new technologies to communicate. It is likely that the pandemic has accelerated the death of distance (Cairncross 1997) but much of this will turn on how we react to the deterrent effect of distance as we have articulated it here. We also need to enrich the analysis with some definite and agreed features that all urban morphologies should meet. For example, limits on trip lengths, densities, and accessibilities all imply different costs and benefits and to embrace this we need to extend

the model. Last but not least, we need to disaggregate the working population into different occupational and industry groups that we know have different work patterns and in this way, we would be able to incorporate a much richer spectrum of heterogeneity than we have been able to present here.

References

Apple (2021) *Mobility Trends Reports*. 31/03/21, https://covid19.apple.com/mobility

Bettencourt, L M A, Lobo, J, Helbing, D, Kühnert, C, and West, G B (2007) Growth, innovation, scaling, and the pace of life in cities. *Proceedings of the National Academy of Science* **104** (17), 7301-7306. https://doi.org/10.1073/pnas.0610172104

Cairncross, F (1997) *The Death of Distance: How the Communications Revolution Will Change Our Lives*. Harvard Business School Press, Boston MA.

Cecchini, A, and Viola, F (1992) *Ficties (Fictitious Cities): Simulation for the Creation of Cities*, Paper presented at the International Seminar on Cellular Automata for Regional Analysis, Dipartimento di Analisi Economica e Sociale del Territorio, Istituto Universitario di Architettura di Venezia, Venice, Italy.

Christaller, W (1933) *Die Zentralen Orte in Siiddeutschland*. Gustav Fischer Verlag Jena, DE, translated in part by C. W. Baskin (1966) *Central Places in Southern Germany*. Prentice-Hall, Englewood Cliffs NJ.

Cochrane, R A (1975) A possible economic basis for the gravity model. *Journal of Transport Economics and Policy* **9**, 34-49.

Coleman, J S (1964) *Introduction to Mathematical Sociology*. The Free Press, Glencoe NY. DOI: 10.1177/0308518X19831591.

Farquharson, C, Rasul, I, and Sibieta, L (2020) *Key Workers: Key Facts and Questions*. Institute of Fiscal Studies, London, accessed 31/10/20, available at https://www.ifs.org.uk/publications/14763

Google (2021) *Community Mobility Reports*. 31/03/21, https://www.google.com/covid19/mobility/

Lowry, I S (1964) *A Model of Metropolis*. RM-4035-RC, The Rand Corporation, Santa Monica CA.

ONS (2020) *Coronavirus and Homeworking in the UK: April 2020: Homeworking Patterns in the UK, Broken Down by Sex, Age, Region and Ethnicity*. 31/03/21 https://www.ons.gov.uk/employmentandlabourmarket/peopleinwork/employmentandemployeetypes/bulletins/coronavirusandhomeworkingintheuk/april2020#measuring-the-data

Schindler, M, Caruso, G (2020) Emerging urban form – emerging pollution: Modelling endogenous health and environmental effects of traffic on residential choice, *EPB: Urban Analytics and City Science* **47**(3), 437–456. DOI: 10.1177/2399808318783206.

Scott, A J (2019) City-regions Reconsidered. *EPA: Economy and Space* **51**(3), 554–580.

Tanner, J C (1961) *Factors Affecting the Amount of Travel*. Technical Paper 5, Road Research Laboratory, London.

Tobler, W (1970) A computer movie simulating urban growth in the Detroit Region. *Economic Geography* **46**, 234–40.

Tobler, W (1976) Spatial interaction patterns. *Journal of Environmental Studies* **6**, 271-301.

Which (2021) *Village Properties in Demand as House Buyers Escape to the Country*, 31/03/21, https://www.which.co.uk/news/2020/08/village-properties-in-demand-as-house-buyers-escape-to-the-country/

Wilson, A G (1971) A family of spatial interaction models, and associated developments. *Environment and Planning **3***, 1-32.

Wurster, C B (1963) The form and structure of the future urban complex. In – L. Wingo Jr., L (Ed) *Cities and Space: The Future Use of Urban Land*. Johns Hopkins Press, Baltimore MD, pp. 73-102.

Supplementary Information

The Post-Pandemic City
Speculation Through Simulation

Defining the Hypothetical City System and Its Model

The hypothetical city consists of N locations, $i, j = 1, 2, 3, \ldots, N$ formed from $n\ x\ n = N$ square cells whose centroids x_i and y_i are defined as

$$x_i = [(i-1) mod\ n] + 1$$

$$y_i = int\left[\frac{(i-1)}{n}\right] + 1 \qquad \text{x} \qquad . \qquad \text{(S1}$$

The distance between any two cells is defined as $d_{ij} = [(x_i - x_j)^2 + (y_i - y_j)^2]^{1/2}$, the minimum distance is 1, and the maximum distance $d_{max} = [(x_1 - x_N)^2 + (y_1 - y_N)^2]^{1/2}$ which is proportional to the areal extent of the city and a bound on the mean trip length in the system. We set the intrazonal distance to $\sqrt{2}/2$ which is approximately proportional to the diameter of each cell; and we assume there is a single central cell defined as $int[(n^2/2) + 1]$ which implies that the number of cells n along each side of the grid and the total N are both odd.

The trip distribution $\{T_{ij}\}$ associated with the origins $\{O_i\}$ and destinations $\{D_j\}$ cannot be visualised in terms of each individual flow as even in this hypothetical application where we keep the number of cells to 121 $(= n^2)$, the number and size of flows is too large to plot and thus we define the dominant direction of flows emanating from every origin to all destinations. The dominant direction of travel in terms of the average of the vectors to all destinations from each given origin are defined from $\sum_j T_{ij}(x_i - x_j) = X_i$ and $\sum_j T_{ij}(y_i - y_j) = Y_i$ and we then compute the direction associated with the coordinate pairs $dx_i = x_i - X_i$ and $dy_i = y_i - Y_i$. We show the grid and these dominant directions by the tiny arrows in Figure S1(a) and this illustrates the perfect symmetry of the system

In the default urban landscape that we define above in the main paper, we impose an hierarchical pattern on the symmetric spatial interaction defined by the model in equation (1) which we show in Figure 1 (main paper). In Figure S1(b), we show a different hierarchy where key hubs are imposed on the periphery of the city and then using an interaction model to predict flows based on $T_{ij} \sim 1/d_{ij}^2$, this largely keeps workers working and living in the same zone. This does break the symmetry of the imposed polycentric hierarchy in Figure 1(c) as reflected in Figure S1(c) but we need to generate very radical changes in the orientation of the system to achieve this as we show in the main paper.

2 4 8

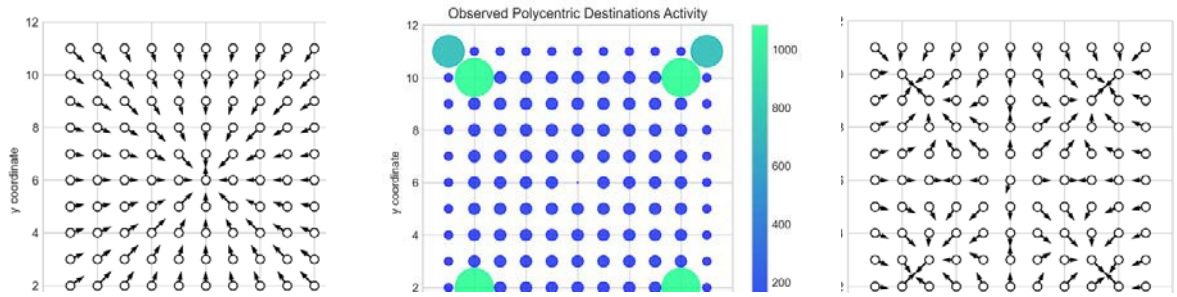

*"#$%&' ?() *+',-./0+'0#123 4&#5 6#0-*

-" #$%'' ('')*, K+4$ 35<+2!24 3+*%:4+52 U%:45*/ -" #$% J+46 K+4$ X,1% J+4+%/ +2 4$% >%*+=$%*6 !2, :" #$% T*5G%2 76<<%4*6 B*5< 4$% A5:!4+52 5E X,1% J+4+%/ +2 -"

F9" *3269$8% $7 +9$% 626"3 92#" 4""7 63:&)8"&)%$7* Q2+65:+5$4 $7 Z;+9:7 27& $+ $% $=6:3+27+ +: =2D" 85"23 +9" >2; +9"; %9:)5& 4" 3"2&? F9" 9;6:+9"+$825 %[]23" *3$& $% 8:=6:%"& :< *,* %[]23" 8"55% >9:%" 8"7+3:$&% 3"63"%"7+ +9" 5:82+$:7% >9$89 >" 2%%:8$2+" >$+9 +9" #:5)="% :< 28+$#$+; c +9" >:3D$7* 6:6)52+$:7 2+ +9"$3 3"%$&"78"% :3 :3$*$7% 9! 27& +9" %2=" 6:6)52+$:7 2+ +9"$3 >:3D6528"% :3 &"%+$72+$:7% :! (55 :)3 =26% :< +9$% *3$& 8$+; 65:+ +9" %$`" :< 28+$#$+; $7 63:6:3+$:7 :: $+% :4%"3#"& :3 63"&$8+"& #:5)="% 2% 2 8$385" 2+ +9" 6:$7+ 5:82+$:7? 0< 27& >9"7 +9" 8$385"% 4"*$7 +: :#"3526- +9"7 2 +327%623"78; 83$+"3$:7 $% $7#:D"& 27& $+ $% 6:%%$45" <:3 +9" 3"2&"3 +: $7+)$+$#"5;)7&"3%+27& +9")7&"35;$7* +3"7&% 25+9:)*9 +9" =:3" +9" 3"2&"3 $% <2=$5$23 >$+9 +9" &2+2 27& +9" %$=)52+$:7%- +9" "2%$"3 $+ $% +: $7+"363"+ +9"%" =26%? F9" %$`" :< "289 6:$7+ $% 42%"& :7 +9" 23"2 :< +9" 2663:63$2+" 8$385"? 0< +9" 28+$#$+; %$`" $% 9! % &JJ)7$+%- <:3 "G2=65"- +9" 23"2 :< +9" 8$385" $% 63:6:3+$:725 +: pO9!p&J? F9" 8:5:)3 $% 25%: 3"52+"& 5$7"235; +: %$`" 4)+ +9" 327*" :< #25)"% #23$"% <:3 "289 =26 %: +92+ +9" =2G$=)= 8:7+32%+ :#"3 +9" 327*" :< #25)"% $% "=65:;"&? E:+" +92+ +9" #:5)="% $7 255 +9"%" =26% 23" %825"& 2)+:=2+$8255; 288:3&$7* +: +9"$3 &"7%$+; 27& 327*" 27& 27; 8:=623$%:7 4"+>""7 =26% 7""& +: +2D" +9$% $7+: 288:)7+?

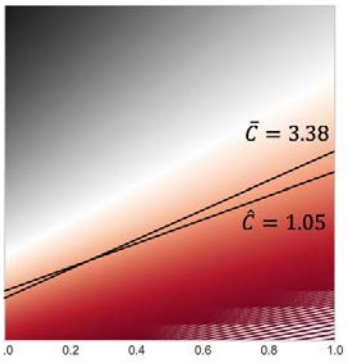

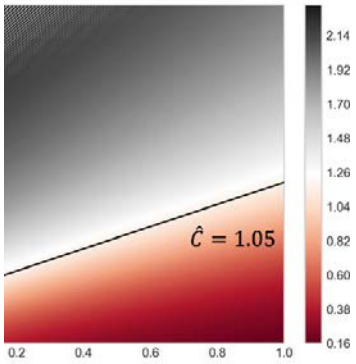

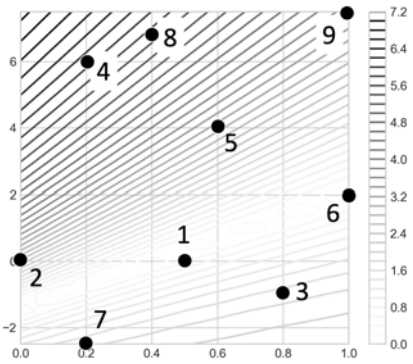

*"#$%&' ?7) K'.&'@'9020#/9@ /A 0+' 82&2='0'& ?.21' 1 B& { C :-#0+ ?2=.3' ?1'92&#/@ K'$#@0'&'5 /9 0+' ?.21' C'A#9'5 H- *&#. L'9$0+ 6/90/%&@*

When we introduce the two parameter gamma function for spatial interaction, we define the parameter space in terms of these parameters $\alpha - 1$ and β. The mean trip length C and the mean of the log of each trip length C^{b} define this space within which we have selected 9 scenarios which reflect very different trip lengths varying from trips between work and home being very local to trips varying across the entire system. In fact, if we have assumed that at the initial lockdown, there is a unique combination of parameter values defined by $C = 3.38$ and $C^{\mathrm{b}} = 1.05$ which are of course hypothetical. We show these trip lengths and their parameters in Figure S2(a) and (b).

The Alternative Scenarios Based on Variants of the Gamma Function

In Figure S3 below, we plot all scenarios associated with the 9 sets of parameter values in Figure 5 of the main paper. These illustrate the ways in which the relative balance between distance as an attractor and as a deterrent to travel led to different concentrations of activity in the hypothetical city.

Scenario 1: $\alpha - 1 = 0,\ \beta = 0.5,\ C = 2.95,\ C^{\mathrm{b}} = 0.91$

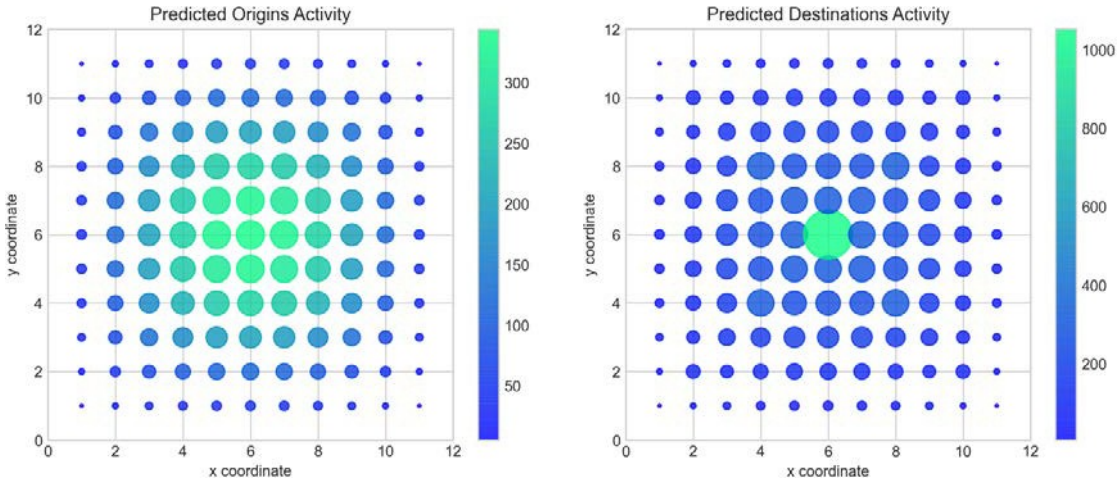

Scenario 2: $\alpha - 1 = 0,\ \beta = 0.0,\ C = 5.43,\ C^{\mathrm{b}} = 1.53$

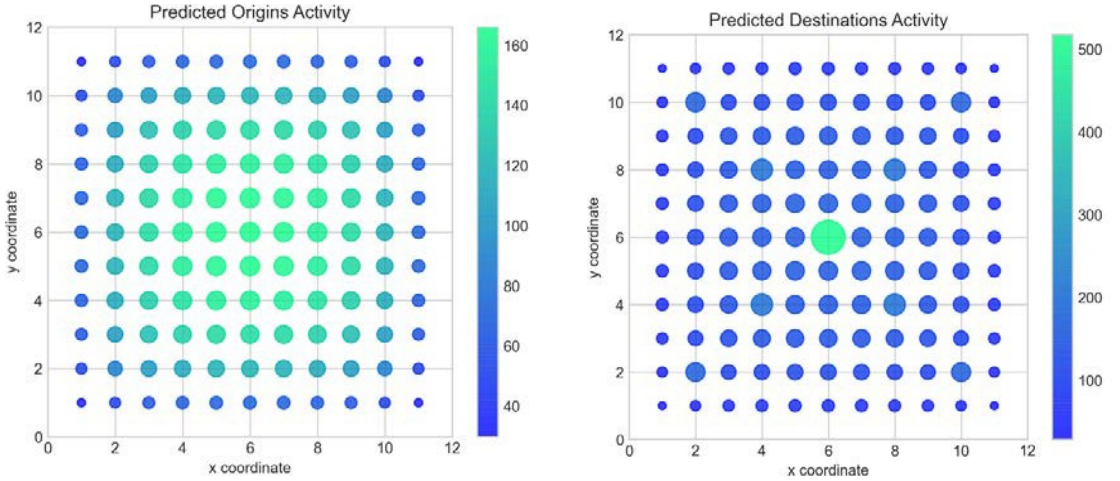

Scenario 3: $\alpha - 1 = -1,\ \beta = 0.8,\ C = 1.71,\ C^{\mathrm{b}} = 0.42$

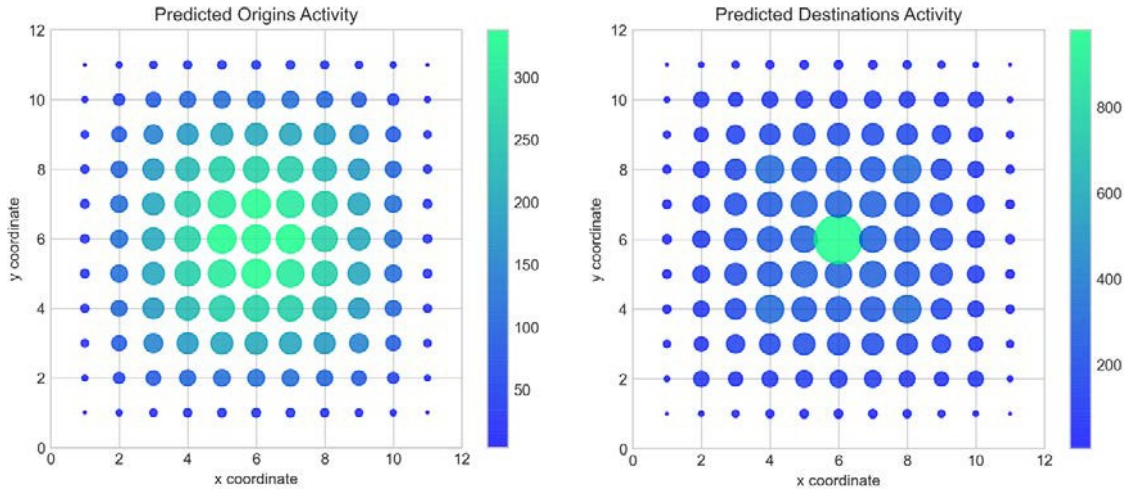

Scenario 4: $\alpha - 1 = 6,\ \beta = 0.2,\ C = 8.86,\ C^{\mathrm{b}} = 2.16$

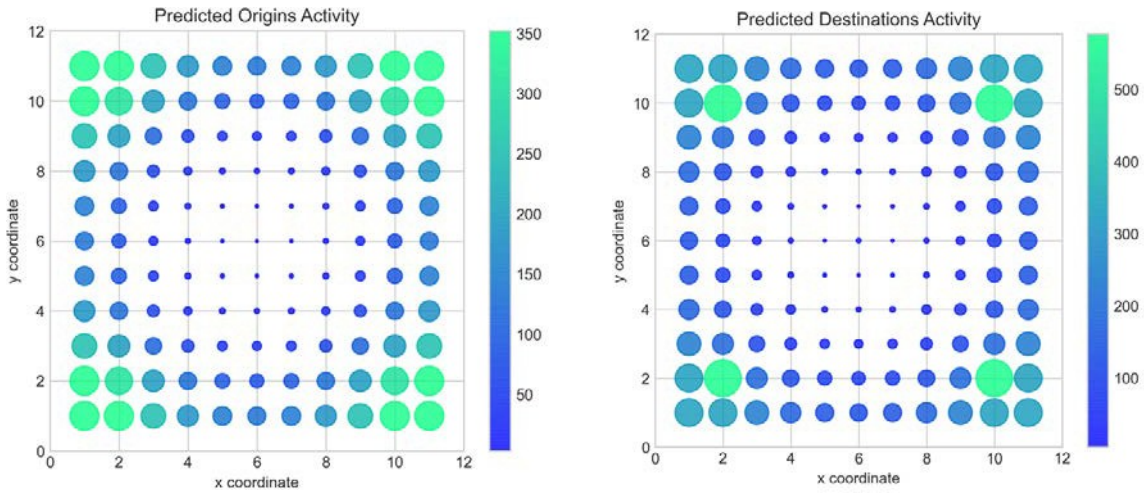

Scenario 5: $\alpha - 1 = 4,\ \beta = 0.6,\ C = 6.17,\ C^{\mathrm{b}} = 1.76$

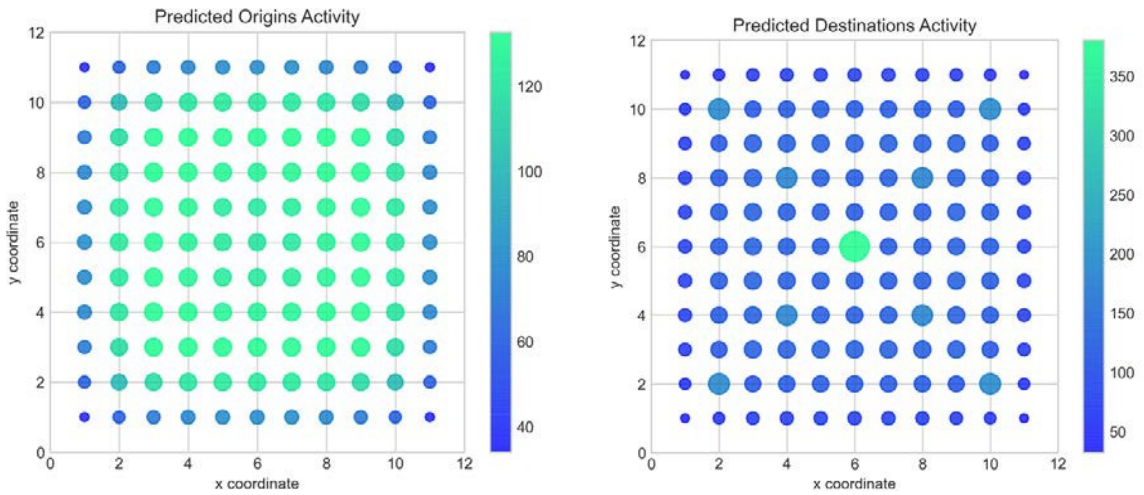

Scenario 6: $\alpha - 1 = 2,\ \beta = 1.0\,,\ C = 3.33,\ C^{\mathrm{b}} = 1.08$

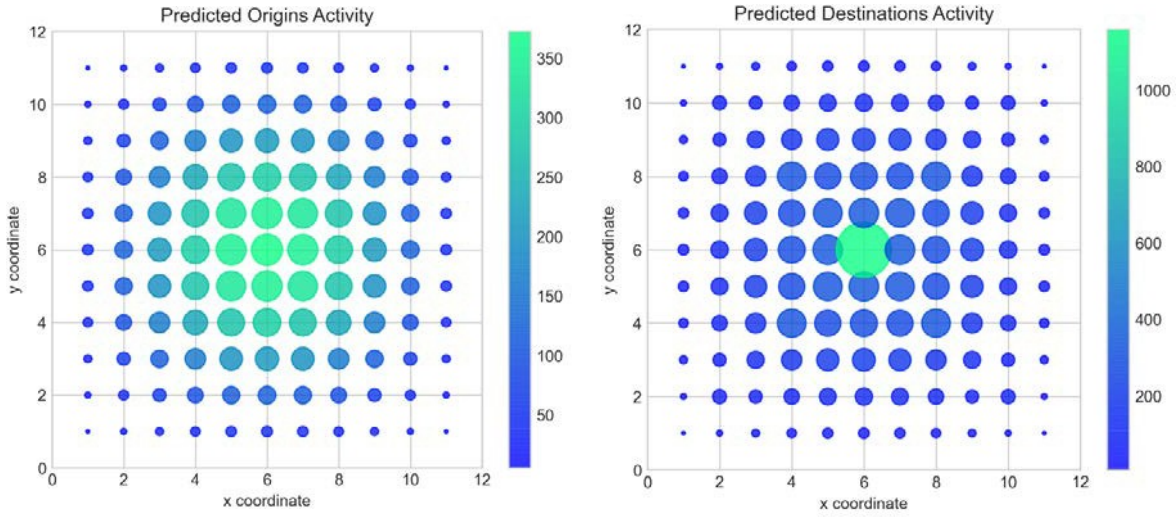

Scenario 7: $\alpha - 1 = -2.5,\ \beta = 0.2\,,\ C = 1.65,\ C^{\mathrm{b}} = 0.37$

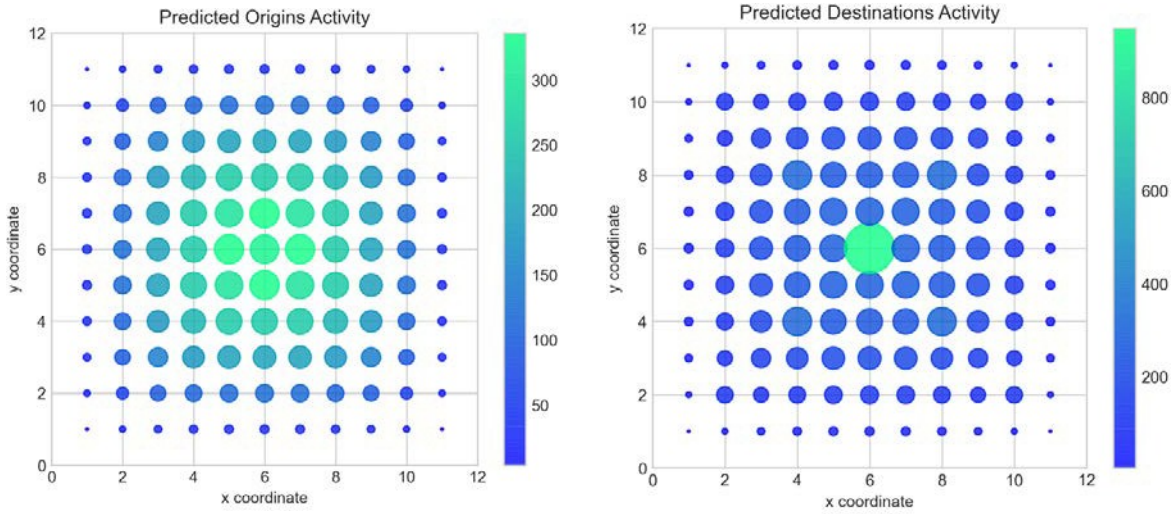

Scenario 8: $\alpha - 1 = 7,\ \beta = 0.4,\ C = 8.59,\ C^{\mathrm{b}} = 2.12$

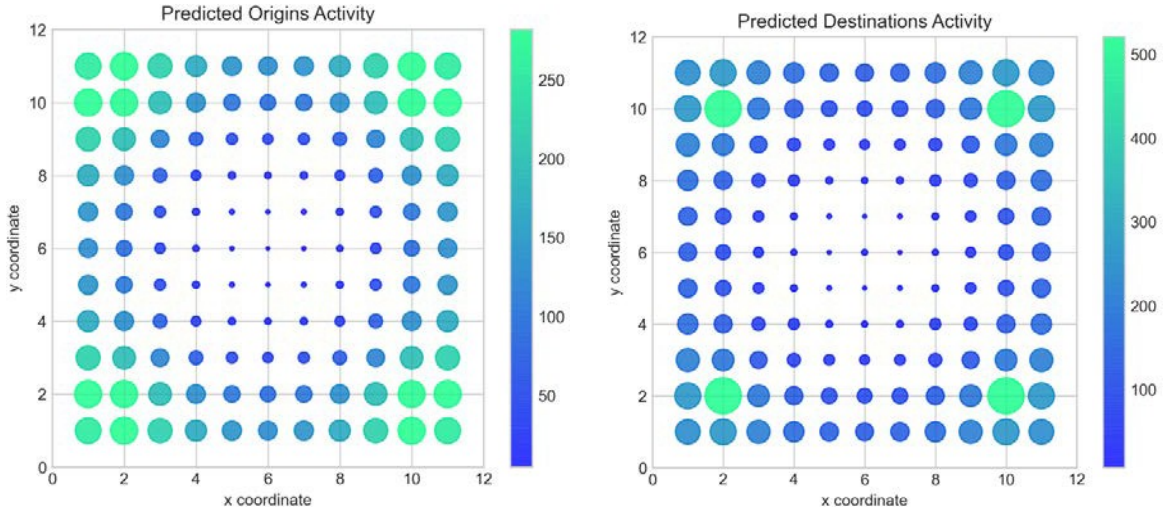

Scenario 9: $\alpha - 1 = 7,\ \beta = 1.0\ ,\ C = 6.78,\ C^{\mathrm{b}} = 1.88$

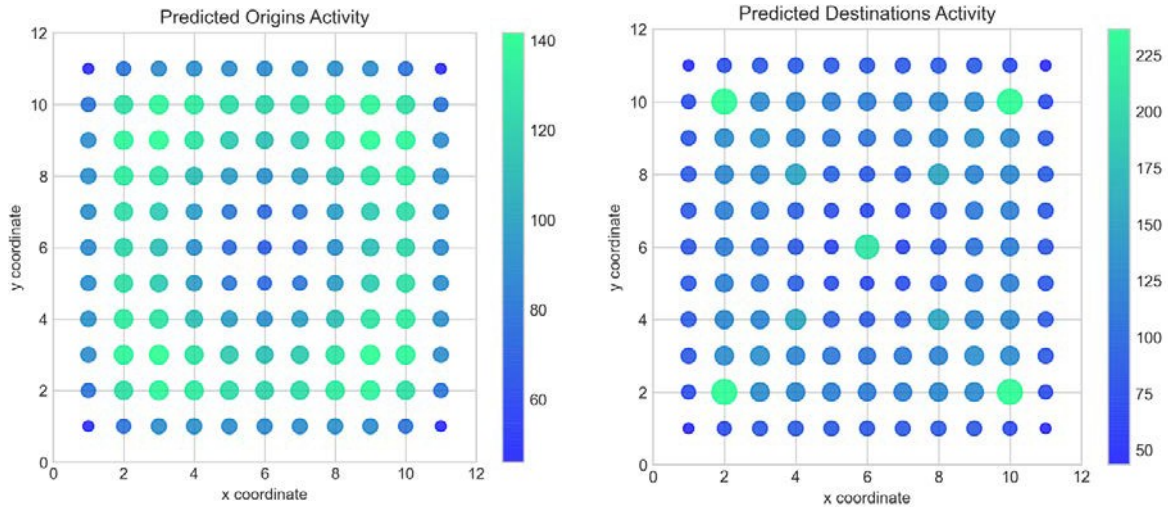

Figure S3: The 9 Scenario Plots for Different Combinations of the Gamma Function

The Release of the Lockdown Based on Increasing λ By Steps of 0.1

In Figure S4, we show the frames for release from lockdown for origins and destination. You could almost cut out the frames and make a flick book from these collages but this gives some idea of the need to experiment with such systems as they are running on the desktop for only then can the essence of this experimental manipulation be appreciated.

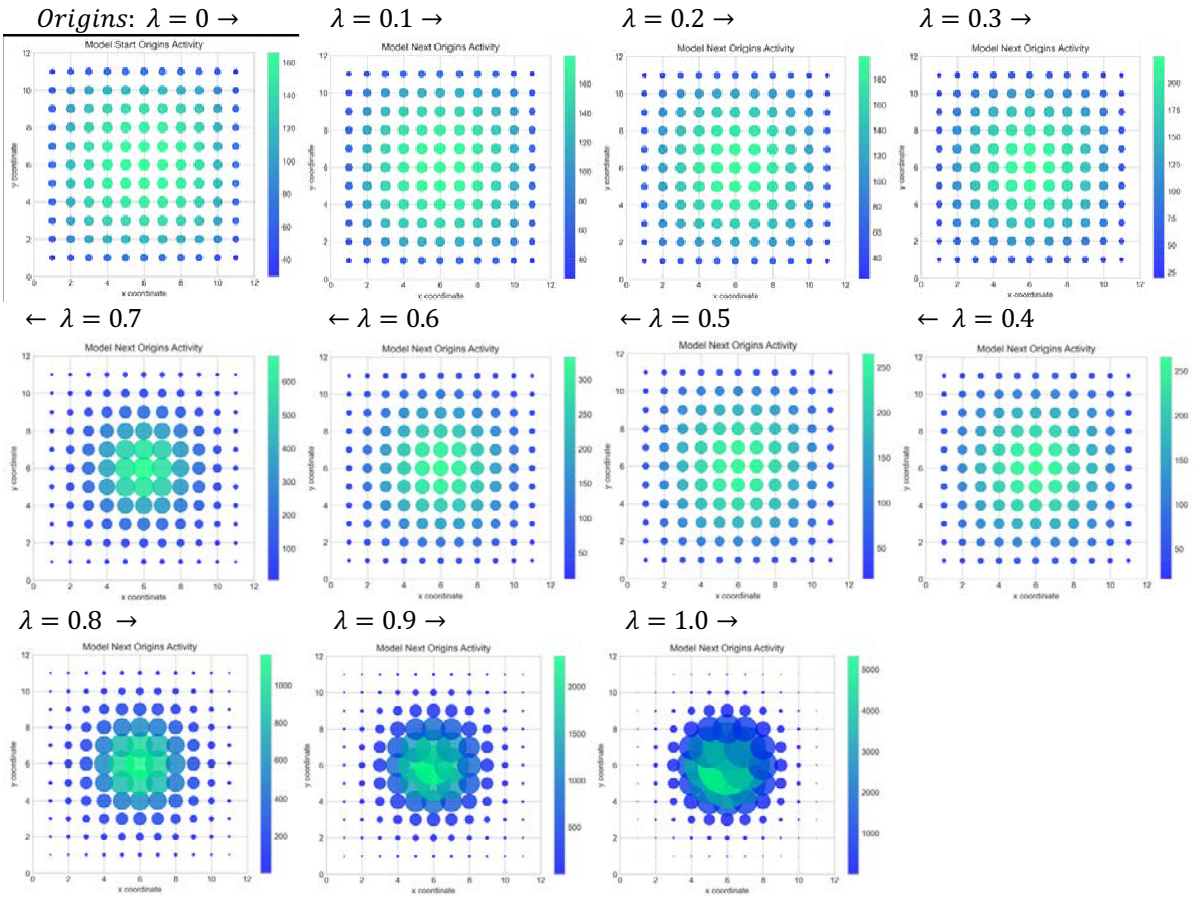

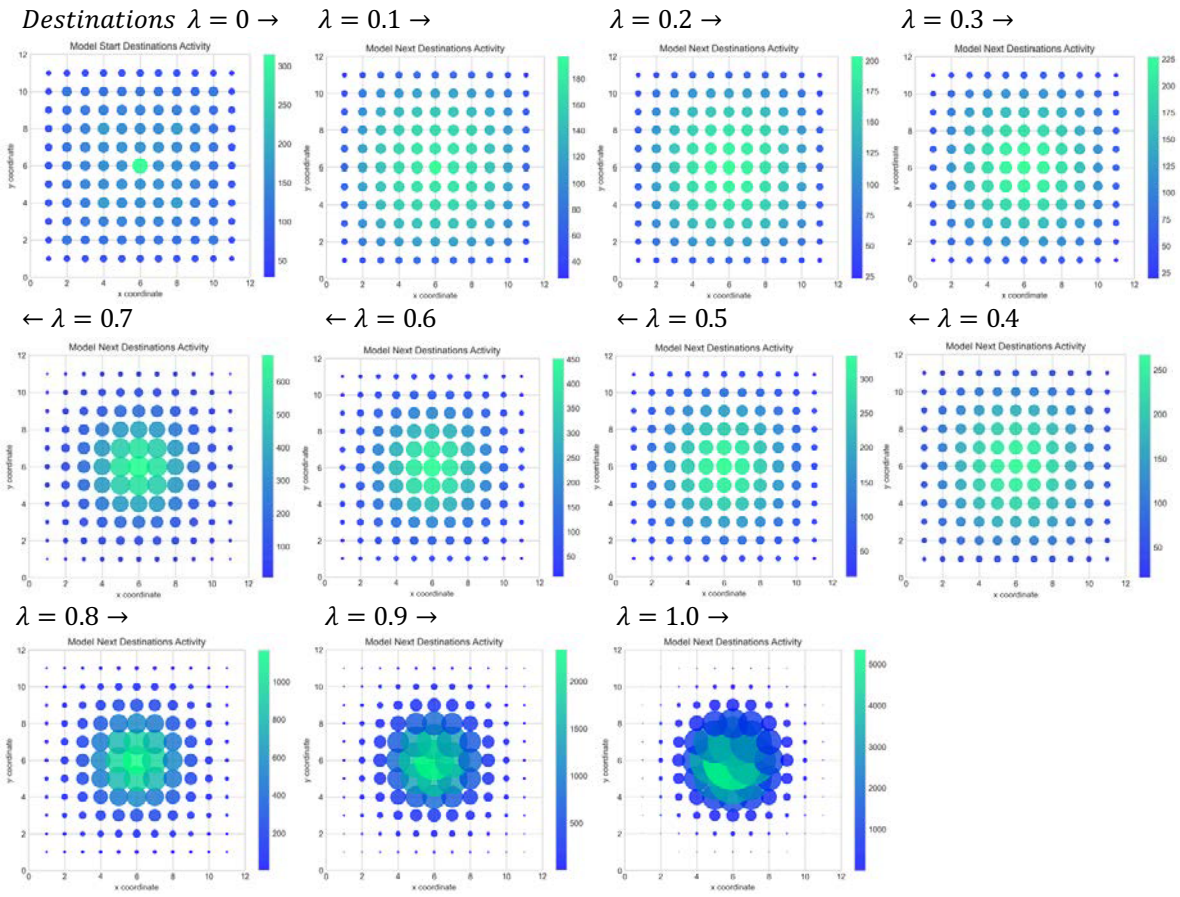

Figure S4: Transitions from Complete Lockdown Back to the Old Normal

Scaling the Hypothetical City Model to the Dimensions of London

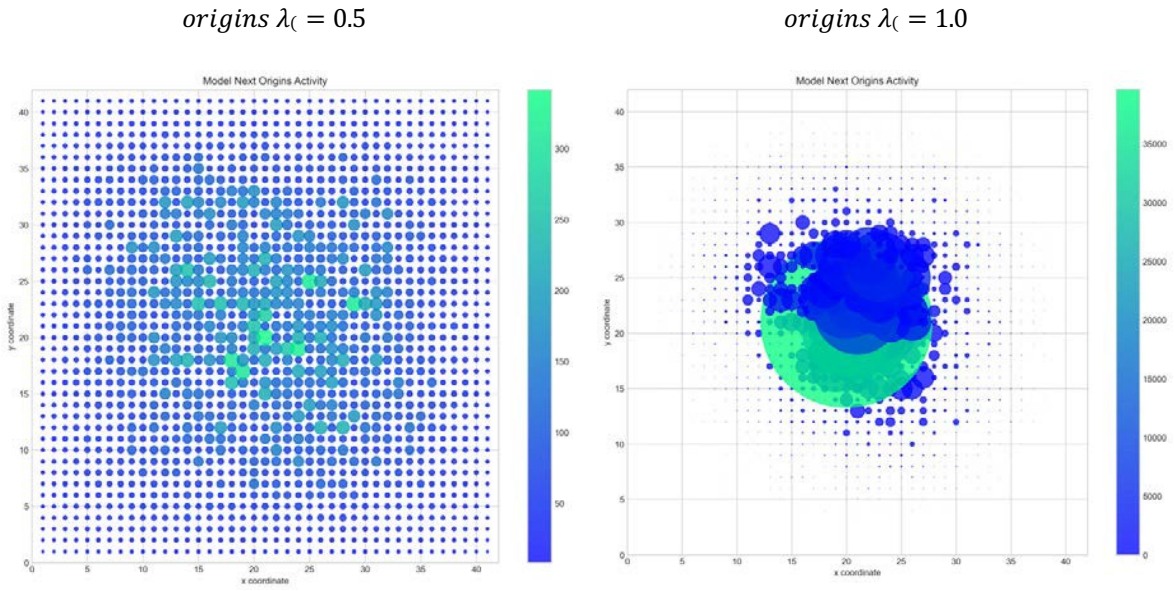

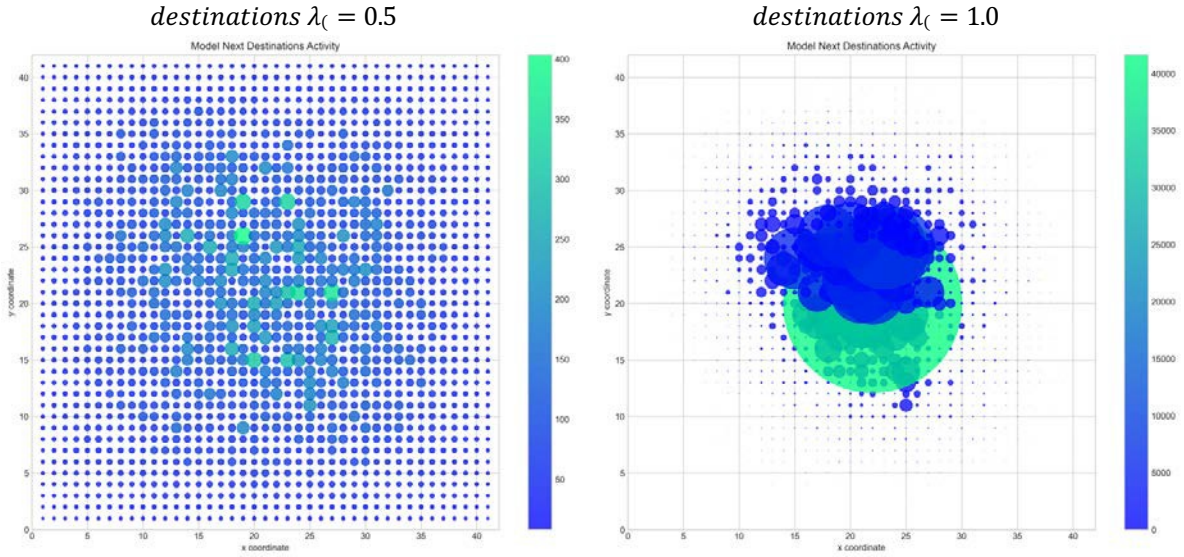

Figure S5: Introducing Randomness and Scaling Up the System from 11x11=121 Zones to 41x41=1681 Zones

Transferring the Model to the London Metropolitan Region

The correlation between the origin and destination data for London is very low at 0.139 and this is indicative of very strong concentration of jobs at the centre of the city. A useful measure of this concentration is the ratio of employment to working population $\varphi = D_{\#}/O_{\#}$ which is also a crude measure of 'excess commuting', that is the number of workers working in the same location in comparison to the population that lives there, in the same location (but do not necessarily working there). The maximum value of this ratio is 1426 in one of the central London zones that has 76822 workers but only 54 residents. In fact, the zone with the greatest concentration of employment at 182693 has a ratio of 44 with the ten largest zones in terms of employment and these ratios are all in the central city. The most effective way of illustrating this difference is by plotting the ratios as we do in Figure S6.

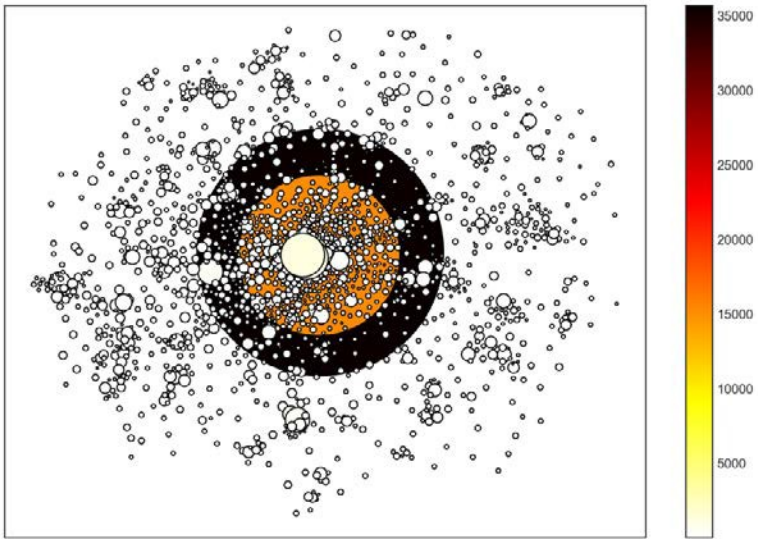

Figure S6: Relative Concentration of Employment to Residential Population $\varphi = D_{\#}/O_{\#}$

This figure shows the very dramatic focus on the centre while at the same time, the local clustering of the polycentric employment hubs that make up the metropolis. The distribution of the residential (origins) and working (destinations) population is given in the main paper as Figures 12(a) and 12 (b) and readers should refer to this to gain a complete picture.

We construct the distributions of origins and destinations that we define as our default by moving $1-\lambda$ from destinations to origins assuming that this proportion of workers work from home. No one changes their residential location where each origin is defined as $O_i = \lambda O_i + (1-\lambda)O_i$ but those now working in terms of their destinations are defined as $D_j = \lambda D_j + (1-\lambda)O_j$. We map these default data in Figure S7 below.

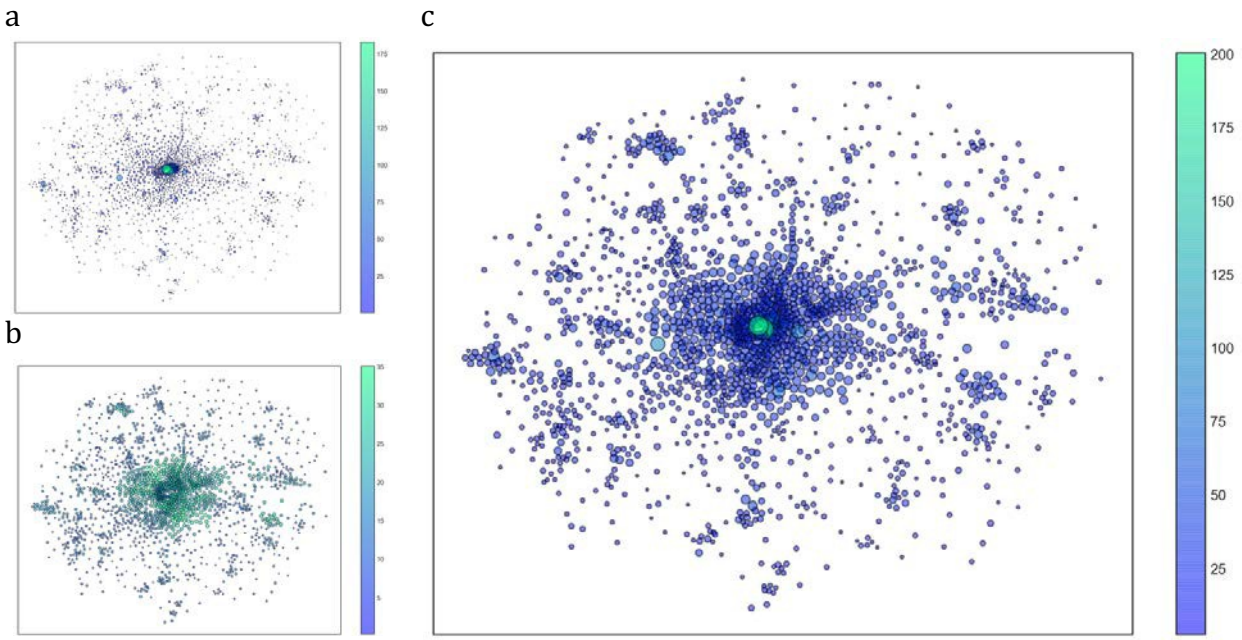

Figure S7: The London Lockdown: 80% Working From Home
a) Essential Workers at Normal Workplace Destinations b) Nonessential Workers Working from Home c) The New Pattern of Workplace Destinations

The Remaining Travel Scenarios

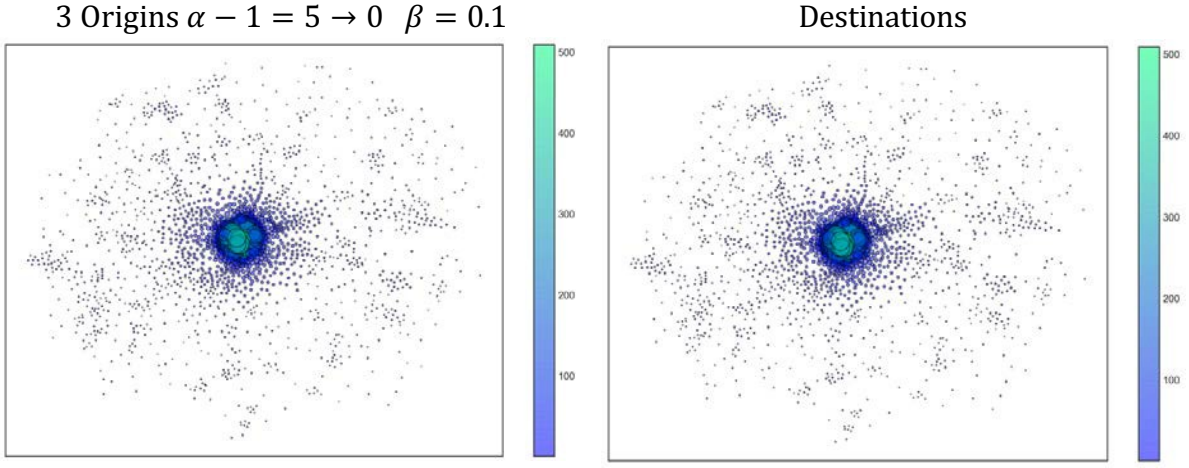

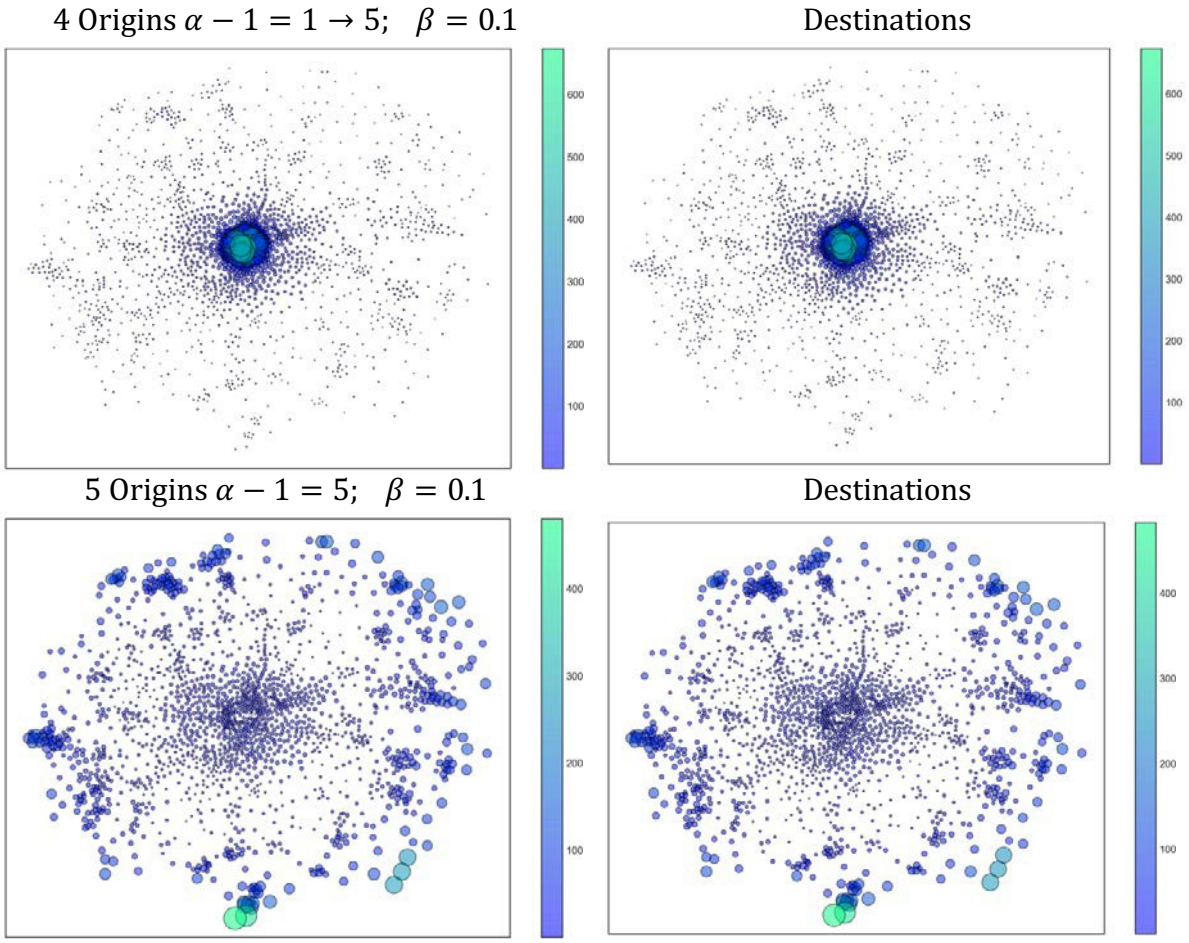

Figure S8: Scenarios 3, 4, and 5 for Recovering from the Lockdown

We also need to portray the degree of heterogeneity using equations (8) and (9) for each of the seven scenarios and we can plot these with respect to changes in the temporal iterations. We illustrate these two graphs in Figure S9. In S9(a), changes from iteration to iteration from equation (8) show substantial changes in travel patterns starting in the first iterations with about 20% different declining to very low differences in heterogeneity as equilibrium is approached. In terms of the cumulative changes using equation (9) from the starting iteration to the equilibrium all scenarios show an increase in heterogeneity up to about 40% by the time the equilibrium is approached with scenario 6 being the most radical with most of the change taking place as soon as the new travel patterns are imposed and then leading to equilibrium very quickly.

The last features illustrated are the directional vectors that define the interaction fields for each of the two extreme Scenarios 6 and 7. There is no focus in the field from Scenario 6 where most activity is drawn to the centre which means that most vectors are randomly focussed as we show in Figure S10. In Scenario 7, the field shows vectors in great tension as half the origin activities are drawn to one edge of the system and the destination activities to the other.

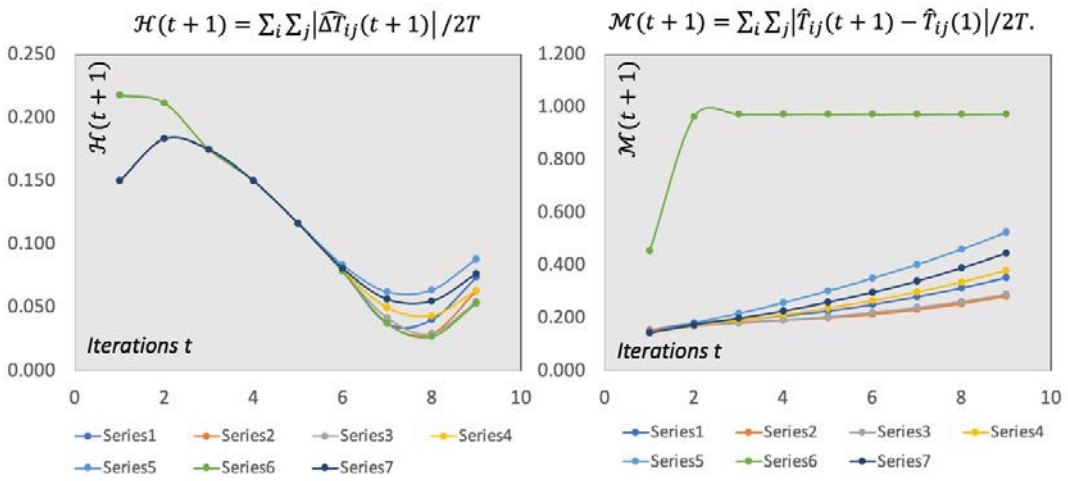

Figure S9 (a) left: Changes From Iteration to Iteration; (b) right: Cumulative Change from the First Iteration

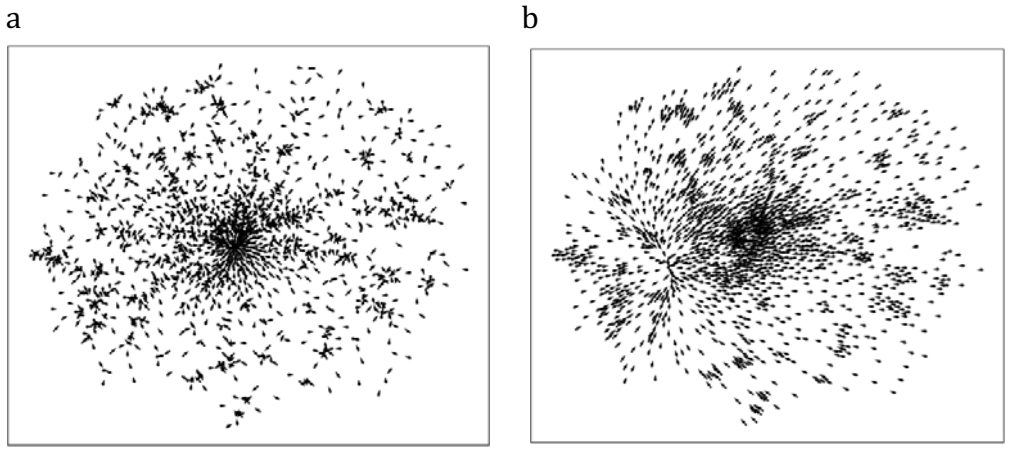

Figure S10: Directional Trip Vectors for Scenarios 6 and 7, after 30 Temporal Iterations

a) Scenario 6 where there is no longer any distinct focus b) Scenario 7 best explained as a field with major attractions south west and east-north east.